INVESTIGATIONS OF TRANSLATIONAL-ROTATIONAL RELAXATIONS IN HYDROGEN ISOTOPES

C. G. SLUIJTER

INVESTIGATIONS OF TRANSLATIONAL-ROTATIONAL
RELAXATIONS IN HYDROGEN ISOTOPES

INVESTIGATIONS OF TRANSLATIONAL-ROTATIONAL RELAXATIONS IN HYDROGEN ISOTOPES

PROEFSCHRIFT

TER VERKRIJGING VAN DE GRAAD VAN
DOCTOR IN DE WISKUNDE EN NATUURWETENSCHAPPEN AAN DE RIJKSUNIVERSITEIT TE LEIDEN OP GEZAG VAN DE RECTOR
MAGNIFICUS DR. D. J. KUENEN, HOOGLERAAR
IN DE FACULTEIT DER WISKUNDE EN
NATUURWETENSCHAPPEN, TEN OVERSTAAN
VAN EEN COMMISSIE UIT DE SENAAT TE
VERDEDIGEN OP WOENSDAG 14 OKTOBER
1964 TE 16 UUR

DOOR

CHRISTOFFEL GIJSBERTUS SLUIJTER

GEBOREN TE ROTTERDAM IN 1932

Promotor: PROF. DR. J. J. M. BEENAKKER

Aan mijn ouders

Het in dit proefschrift beschreven onderzoek werd uitgevoerd als onderdeel van het programma van de Werkgemeenschap voor Molecuulfysica van de Stichting voor Fundamenteel Onderzoek der Materie (F.O.M.) met financiële steun van de Nederlandse Organisatie voor Zuiver Wetenschappelijk Onderzoek (Z.W.O.).

Teneinde te voldoen aan het verzoek van de Faculteit der Wiskunde en Natuurwetenschappen volgt hier een overzicht van mijn studie.

Na beëindiging van mijn middelbare-schoolopleiding in 1950 aan de 4e Gemeentelijke H.B.S. (thans Willem de Zwijger H.B.S. geheten) te Rotterdam begon ik mijn studie aan de Rijksuniversiteit te Leiden. In 1953 legde ik het candidaatsexamen d in de wis- en natuurkunde met bijvak scheikunde af. Hierop volgde in 1956 het doctoraal examen in de experimentele natuurkunde met bijvak netwerkanalyse. Inmiddels was ik sinds 1953 werkzaam in de groep voor molecuulfysica van het Kamerlingh Onnes Laboratorium. Hiertoe in staat gesteld door een studiebeurs verleend door de Gemengde Technische Commissie ter Uitvoering van het Nederlands-Belgisch Cultureel Accoord, was ik gedurende de zomers van 1955 en 1956 een aantal maanden werkzaam op het Instituut voor Lage Temperaturen en Technische Fysica te Leuven. Na het vervullen van mijn militaire dienstplicht was ik opnieuw in het Laboratorium te Leuven werkzaam. Ik werkte aldaar aan de ontwikkeling van een akoestische thermometer onder leiding van Prof. Dr. A. van Itterbeek, directeur van dit laboratorium. In september 1958 begon ik op het Kamerlingh Onnes Laboratorium te Leiden onder leiding van Prof. Dr. A. van Itterbeek en Dr. J. J. M. Beenakker aan een onderzoek over de rotatie-translatie relaxatie in waterstof-isotopen. Van 1959 tot september 1964 was ik wetenschappelijk medewerker van de Stichting voor Fundamenteel Onderzoek der Materie en werkzaam in de Werkgroep voor Molecuulfysica. Na het vertrek van Prof. Dr. A. van Itterbeek berustte de leiding van de Werkgroep voor Molecuulfysica by Prof. Dr. K. W. Taconis en Prof. Dr. J. J. M. Beenakker.

Van 1959 tot september 1964 was ik tevens leraar aan de avondcursus V.M.T.O.-U.T.O. van de Academie voor Beeldende Kunsten en Technische Wetenschappen te Rotterdam. Sinds september 1964 ben ik verbonden als wetenschappelijk medewerker aan het Natuurkundig Laboratorium der N.V. Philips' Gloeilampenfabrieken te Eindhoven.

Het in dit proefschrift beschreven onderzoek werd verricht in samenwerking met achtereenvolgens de heren J. Dussel, J. J. S. F. de la Rie en R. M. Jonkman. Technische hulp werd verleend door de verschillende leden van de vaste staf van het Kamerlingh Onnes Laboratorium, in het bijzonder door de heren J. M. Verbeek voor de constructie van het in dit proefschrift beschreven toestel, T. Nieboer voor het cryogene werk en J. Rol voor het elektronische werk. De discussies met Dr. H. F. P. Knaap droegen zeer tot het totstandkomen van dit proefschrift bij.

CONTENTS

CHAPTER I

DETERMINATION OF ROTATIONAL RELAXATION TIMES OF HYDROGEN ISOTOPES BY SOUND ABSORPTION MEASUREMENTS

Summary

An apparatus to measure sound absorption at low temperatures is described. Measurements were performed on hydrogen isotopes at 77, 90 and 293°K to determine the excess absorption due to relaxation between the rotational and translational energy states. For p-H_2 and o-D_2 at 77 and 90°K an absorption curve was found which could be fitted with the theoretical curve of a process with a single relaxation-time. Hence in this case the relaxation times could be determined uniquely. In Chapter III the experimental results will be discussed and compared with theoretical investigations based on calculations of the cross-section for rotational transitions.

1. *Introduction.* From experiments on equilibrium and transport properties in gases little information can be obtained on the non-spherical part of the intermolecular potential. At the most one arrives at an estimate of its magnitude. A more direct approach is needed to get reliable data. This can be done by studying the rotational-energy transfer in molecular collisions through sound absorption measurements as the energy transfer depends strongly on the non-spherical part of the interaction between the molecules. For theoretical analysis of experimental results molecules with only two occupied rotational states are most suited. Such a two-level system can be found in hydrogenic molecules at low temperatures as was already pointed out by Rhodes [1]). The very small moments of inertia of these molecules give rise to large spacing of the rotational-energy levels.

Hence in gaseous hydrogen one can arrive at a situation in which only two levels are important. This occurs at temperatures between 20 and 150°K depending on the isotopic constitution of the molecules. The delay in energy exchange between the rotational and translational degrees of freedom causes relaxation phenomena and hence an excess absorption in a sound wave. For H_2 this was first detected by Van Itterbeek and coworkers [2]) [3]) [4]). The most reliable method to obtain the relaxation time from sound absorption measurements is to determine the frequency at which the excess absorption passes through its maximum. Such measurements, however, have not been performed at temperatures low enough to study a two-level system. Therefore we constructed an apparatus suited for low temperatures, based on the progressive-wave method. The method consists in measuring the decay in pressure of a progressive-sound wave as a function of distance from the transmitter. Following Meyer and Sessler 5) we used condenser transducers with a solid dielectric.

In this Chapter measurements are reported on para H_2 and ortho D_2 at 77, 90 and 293°K and on normal H_2, normal D_2 and HD at 77 and 293°K. Values of the measured relaxation times will be compared with theoretical considerations in Chapter III

2. *Experimental method.* For sound absorption measurements several methods are used. It can be shown (cf. section 3) that at low enough densities measurements of the sound absorption as a function of pressure p at constant frequency f give the same result as measurements as function of frequency at constant pressure. In other words the relaxation absorption is a function of f/p only. We performed our measurements mainly as function of pressure since it is experimentally easier to vary the pressure instead of the frequency to cover a large f/p range. As the maximum of the excess absorption in hydrogenic molecules occurs at about 10 MHz/atm the progressive-wave method is the most appropriate one (see ref. 6).

This method is illustrated in fig. 1. A piston source of radius a (fig. 1a)

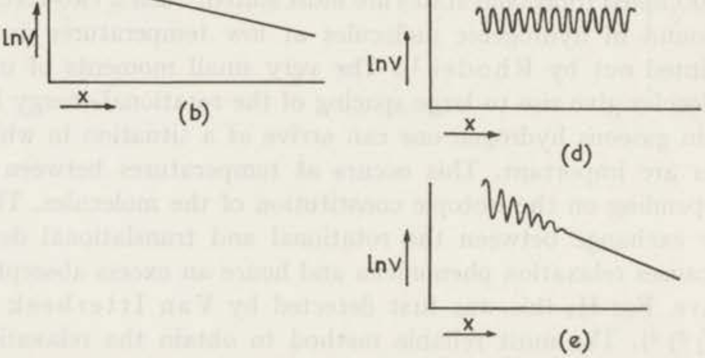

Fig. 1. Measurement of sound absorption by the progressive-wave method. V amplitude of the sound wave.

generates a sound wave of wavelength λ. To a distance a^2/λ the sound field is confined in a cylinder of radius a. The amplitude of the sound wave, averaged over a cross-section of this cylinder, decreases exponentially with the distance from the sound source through absorption in the medium (fig. 1*b*).

The average amplitude can be measured by placing a sound detector with an area equal to that of the source in the cylindrical sound field (fig. 1*c*). This will however disturb the sound field due to reflection from the surface of the receiver. This gives rise to interference phenomena (fig. 1*d*). At high enough absorption in the medium this effect will be negligible at larger distances (fig. 1*e*). In this case an exponential decrease of the amplitude with distance will be found by moving the detector through the sound field. We will now give a more detailed discussion of the experimental arrangement treating successively the transducers, the mechanical part and the electronical part.

a. Transducers. Receiver and transmitter are of the condenser type with solid dielectric as developed by Kuhl, Schodder and Schröder 7). These transducers have the advantage over crystals of being applicable over a large continuous frequency range, in our case up to 0.5 MHz. As they are not driven at their proper frequency, sound transmitter and receiver have not to be tuned to the same frequency. This is of importance when measurements are performed at different temperatures, because tuned elements often show a frequency shift when the temperature changes. Furthermore they have the advantage of giving low mechanical and electrical cross-talk. Fig. 2 gives a schematic diagram of the transducers which were developed for use at low temperatures, while fig. 3 shows the different parts. The main difference with the original design of Kuhl *e.a.* is a springloaded backplate, which is necessary to maintain a constant stress in the foil when cooling it.

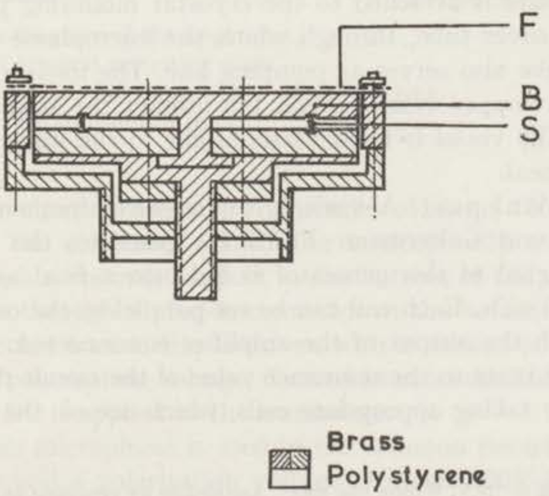

Fig. 2. Schematic diagram of the transducer. *F* foil, *B* backplate, *S* spring.

As vibrating foil metallised condensor paper, furnished by Bosch Germany was used *). Paper foils proved to be more reliable and more sensitive than polystyrene foils.

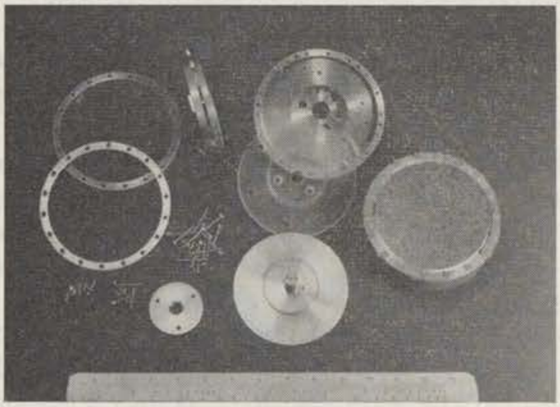

Fig. 3. The different parts of the transducer.

b. Mechanical part. The mounting of the transducers is shown in figs. 4 and 5. The transmitter is mounted at the lower end of the apparatus in such a way that the surface can be set parallel to that of the receiver by means of adjustment screws. The receiver is movable by means of a german silver tube that passes through an O-ring seal in the top of an other wider german silver tube ending in the cryostat mounting-plate.

The distance between receiver and transmitter can be varied between 0 and 17 cm. This is done by moving the receiver at uniform speed by means of a motor and gearbox.

The upper plate is attached to the cryostat mounting plate by means of the german silver tube, through which the microphone driving tube is guided. This tube also serves as pumping line. The measuring space itself is formed by a copper vessel, which fits around the transmitter and receiver frame. The vessel is fixed vacuumtight to the upper plate with an indium O-ring seal.

c. Electronical part. A variable carrier-wave frequency transmitter (type Wandel und Goltermann TFPS 75) generates the measuring frequency. The signal of this generator is fed into a final amplifier, which contains several coils. Each coil can be set parallel to the condensor transmitter, to which the output of the amplifier is connected. The frequency of the generator is set to the resonance value of the circuit that is obtained in this way. By taking appropriate coils, which are of the potcore type,

---

*) We are indebted to "N.V. Willem van Rijn", Amsterdam for providing us with the metallised condenser-paper.

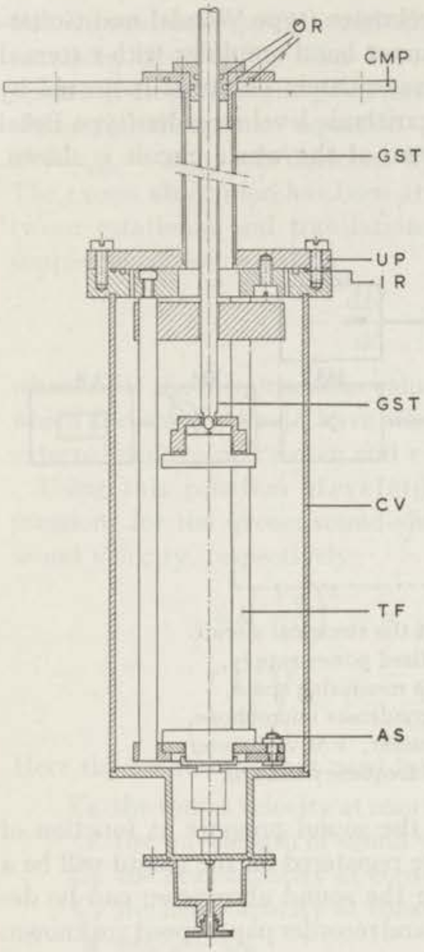

Fig. 4. Schematic diagram of the apparatus.
OR O-ring, *CMP* cryostat mounting plate,
GST german silver tube, *UP* upper plate, *IR* indium ring,
CV copper vessel, *TF* transmitter frame,
AS adjustment screws.

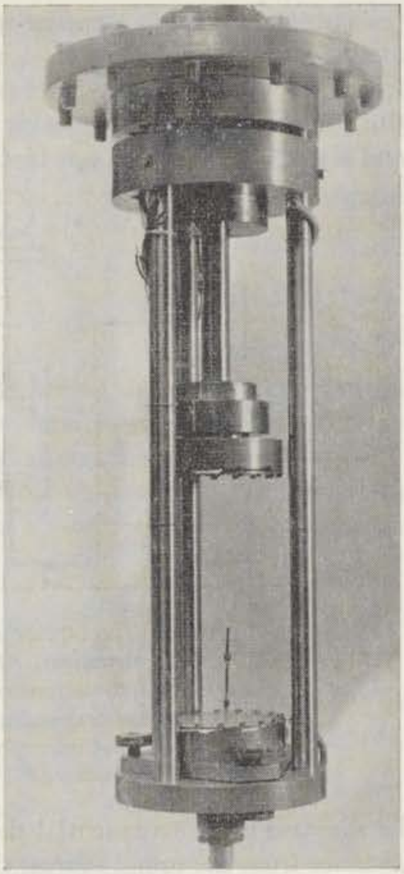

Fig. 5.
The experimental arrangement.

it is possible to choose measuring frequencies of about 100, 200, 300, 400 and 500 kHz. The condenser transmitter is electrically connected to the amplifier through a vacuum support in the bottom of the vessel. The connection is made through a plug-in connector at the bottom of the vacuum can. The condenser transmitter is driven with a voltage of maximal 50 V. Furthermore a polarisation voltage, derived from a stabilized power supply of about 100V DC is applied to the transmitter.

The condenser microphone is used in the common electrical circuit with load resistance and a polarisation voltage of about 100V DC. The microphone signal is non-selectively amplified in a preamplifier, from which the output is fed into a carrier-wave levelmeter (type Wandel und Goltermann TFPM 76). This is a selective narrow band amplifier with external frequency control by the carrier-wave transmitter. The level indicated by this meter is registered by means of a logarithmic level recorder (type Brüel and Kjaer 2340). In fig. 6 a block diagram of the whole circuit is shown.

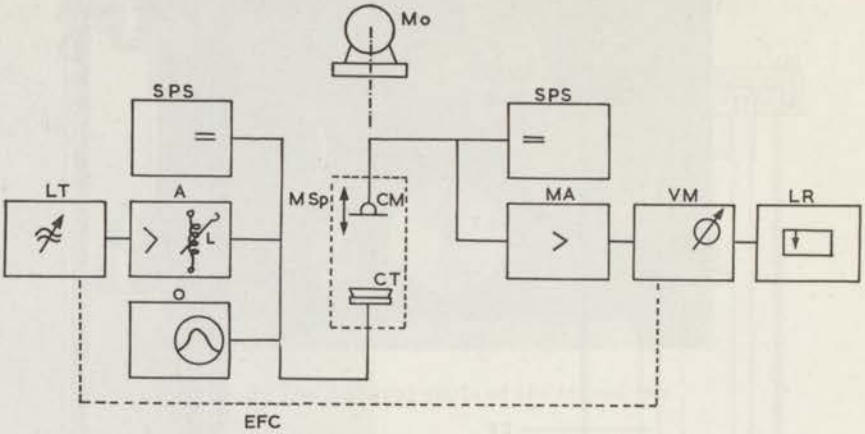

Fig. 6. The block diagram of the electrical circuit.
LT level transmitter, *SPS* stabilized power supply,
A amplifier, *O* oscilloscope, *MSp* measuring space,
CT condenser transmitter, *CM* condenser microphone,
Mo motor, *MA* microphone amplifier, *VM* volt meter,
LR level recorder, *EFC* external frequency control.

In the case of an exponential decay of the sound pressure as function of distance from the sound source, the curve registered on the record will be a straight line. From the slope of this line the sound absorption can be determined when microphone driving-speed and recorder paper speed are known.

3. *Experimental results and discussion.* Absorption of sound in fluid media has first been treated by Kirchoff[8]) and Stokes[9]). They derived an expression for the so called classical sound absorption α_{class} by taking into account energy losses due to viscosity and heat conductivity:

$$\alpha_{\text{class}} = \frac{2\pi^2}{\gamma p V} \left\{ \frac{4}{3}\eta + \frac{\gamma - 1}{c_p} \lambda \right\} f^2 \tag{1}$$

where η is the shear viscosity
λ the coefficient of heat conductivity
c_p the heat capacity at constant pressure
c_v the heat capacity at constant volume
V the sound velocity
γ the ratio c_p/c_v
p the static pressure
f the frequency of the sound wave.

For monoatomic gases sound absorption according to equation (1) was found by Keller[10]), Van Itterbeek and Verhaegen[4]) and Greenspan[11]). In polyatomic gases however, the absorption, is much larger than seems to follow from equation (1). In hydrogen this excess absorption $\alpha' = \alpha_{\text{exp}} - \alpha_{\text{class}}$ was detected by Van Itterbeek and coworkers[2]) [3]) [4]). The excess absorption has been attributed to a slow exchange of energy between rotational and translational degrees of freedom. One can use the simple relaxation equation:

$$-\frac{dE'}{dt} = \frac{1}{\tau}\,[E' - E'\,(T_{\text{tr}})], \tag{2}$$

where E' is the instantanious value of the internal energy, $E'(T_{\text{tr}})$ the value which the energy would have when the system is in equilibrium with the external degrees of freedom and τ the relaxation time.

Using this equation Herzfeld and Rice[12]) derive the following expressions for the excess sound-absorption α' and for the dispersion in the sound velocity, respectively:

$$\alpha'\lambda\left(\frac{V_0}{V}\right)^2 = \pi\,\frac{\Delta C'}{C_v(C_p - C')}\,\frac{\omega\tau'}{1 + \omega^2\tau'^2} \tag{3}$$

$$\left(\frac{V_0}{V}\right)^2 = 1 - \frac{\Delta C'}{C_v(C_p - C')}\,\frac{\omega^2\tau'^2}{1 + \omega^2\tau'^2}. \tag{4}$$

Here the notation is that used by Herzfeld and Litovitz[13]), *i.e.*

V_0 the sound velocity at zero frequency
λ the wavelength of sound wave
C_p the heat capacity at constant pressure per mole
C_v the heat capacity at constant volume per mole
$\Delta = C_p - C_v$,
C' the rotational specific heat per mole
$\omega = 2\pi f$ and

$$\tau' = \frac{C_p - C'}{C_p}\,\tau.$$

From formulae (3) and (4) it follows that:

$$\alpha'/f = \frac{1}{V_0}\left(1 - \frac{\Delta C'}{C_v(C_p - C')}\,\frac{\omega^2\tau'^2}{1 + \omega^2\tau'^2}\right)^{-\frac{1}{2}}\pi\,\frac{\Delta C'}{C_v(C_p - C')}\,\frac{\omega\tau'}{1 + \omega^2\tau'^2}. \tag{5}$$

In formulae (3), (4) and (5) τ' always occurs in the combination $\omega\tau'$, therefore the sound absorption in gases only depends on $\omega\tau'$. Under the assumption that transitions between rotational and translational energy states are only caused by binary collisions, the relaxation times τ' will be proportional to the collisionrate and hence to $1/p$. Thus the absorption can also be measured as a function of f/p, where f/p differs from $\omega\tau'$ only by a constant factor independent of pressure and frequency. The absorption curve for a single relaxation time process as given by equation (3) has a uniform shape independent of the value of τ' and the factor

$$\frac{\Delta C'}{C_v(C_p - C')}$$

if $\alpha'\lambda(V_0/V)^2$ is plotted on a double logarithmic scale as a function of $\omega\tau'$ or f/p. By plotting the experimental points in this way, one can determine easily whether only one or more relaxation times are involved. This is done by moving a transparency with the single relaxation time curve over the measured points. If different relaxation times are present the measured points will lie on a broader curve. In case, however, that the measured points lie on the theoretical one-relaxation-time curve this can be verified by the present method in a rather accurate way.

Such a situation is found for the hydrogen isotopes if one works in a suitable temperature range. The molecules behave as rigid rotators with an energy spectrum

$$E_J = J(J+1)\kappa\theta \text{ with}$$

$$\theta = \frac{h^2}{8\pi^2 I\kappa},$$

J rotational quantum-number, κ Boltzmann's constant, h Planck's constant and I the moment of inertia. Because of the small value of the moment of inertia the energy-level spacing is very large. (The characteristic temperatures θ are 84.8, 63.8 and 42.6°K for H_2, HD and D_2 resp. [14])). The situation is somewhat more complicated for the homonuclear molecules by the occurrence of two modifications depending on the total nuclear spin of the molecule, the so-called ortho- and para H_2 and D_2. This arises from the fact that the symmetry conditions imposed on the total wave function of the molecule, combined with the symmetry properties of the total nuclear-spin allow only certain rotational levels to be occupied. Thus one has for hydrogen: para hydrogen with total nuclear-spin 0 and even rotational states ($J = 0, 2$ etc.) and ortho hydrogen with total nuclear spin 1 and odd rotational states ($J = 1, 3$, etc.). At high temperatures (room temperature) the ortho modification is (by definition) the most abundant one, and one has the so-called normal composition 75% ortho and 25% para for H_2 and $66\frac{2}{3}$% ortho and $33\frac{1}{3}$% para for D_2. Transitions between the two modifications are forbidden and are only obtained by means of a catalyst. This has several consequences. First for H_2 and D_2 the ortho-and para modifications can be treated as two distinct gases and in the second place the energy jumps are larger because only transitions with $\Delta J = 2$ are allowed.

Since HD is a heteronuclear molecule no symmetry conditions are imposed on its wave function. Therefore HD has no ortho- and para-modifi-

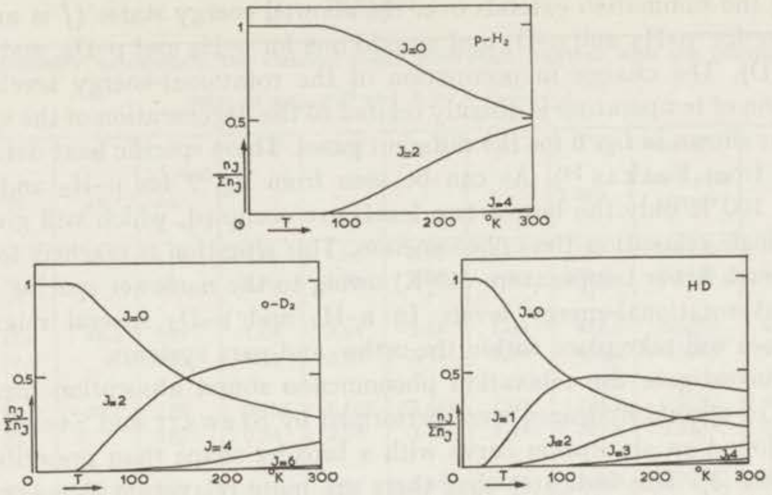

Fig. 7. The occupation of the rotational-energy levels as a function of temperature for p–H_2, o–D_2 and HD.

cations, so that transitions with $\Delta J = 1$ are allowed. To illustrate the behaviour of the hydrogen isotopes and their modifications the occupation of the different rotational levels is given as a function of temperature in fig. 7. The fraction $n_J/\sum n_J$ of the total number of molecules that is in an energy state $E_J = J(J+1)\,\kappa\theta$ is given by

$$\frac{n_J}{\sum n_J} = \frac{(2J+1)\exp\left(\dfrac{-J(J+1)\kappa\theta}{\kappa T}\right)}{\sum_J (2J+1)\exp\left(\dfrac{-J(J+1)\kappa\theta}{\kappa T}\right)}$$

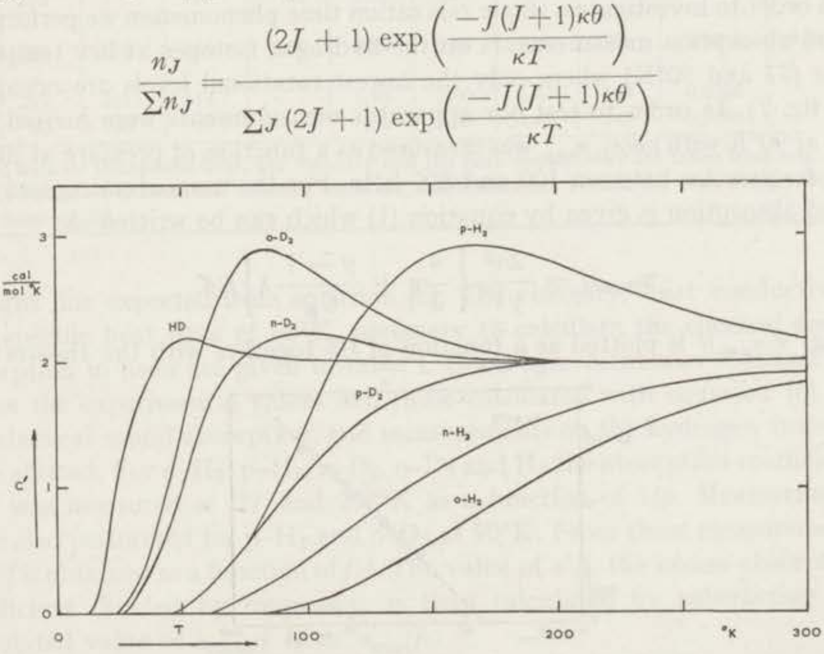

Fig. 8. The rotational specific heat of different hydrogen isotopes and their modifications.

where the summation extends over the allowed energy states (J is an even integer for p–H_2 and o–D_2 and an odd one for o–H_2 and p–D_2, and either for HD). The change in occupation of the rotational-energy levels as a function of temperature is directly related to the degeneration of the specific heat as shown in fig. 8 for the different gases. These specific heat data were taken from Farkas [14]). As can be seen from fig. 7 for p-H_2 and o–D_2 below 100°K only the lowest two levels are occupied, which will give rise to a single relaxation time phenomenon. This situation is reached for HD at a much lower temperature (40°K) owing to the narrower spacing of the allowed rotational-energy levels. In n–H_2 and n–D_2 several relaxation processes will take place within the ortho- and para systems.

To investigate the relaxation phenomenon sound absorption measurements in normal hydrogen were performed by Stewart and Stewart [15]). They found an absorption curve with a broader shape than prescribed by equation (3). This indicates that there are more relaxation times present, corresponding to different transitions within the ortho- and parasystems. Hence Geide [16]) investigated pure p–H_2 at room temperature, where only the three rotational levels ($J = 0,2$ and 4) are important (see fig. 7). From his absorption curve he calculates two relaxation times, one referring to the 0–2 and the other to the 2–4 transition. As the relaxation times are not far apart it is difficult to determine them uniquely from the measured curve alone, as was also shown in general by Beyer [17]).

In order to investigate a single relaxation time phenomenon we performed sound absorption measurements on the hydrogen isotopes at low temperatures (77 and 90°K) where only the lowest rotational levels are occupied (see fig. 7). In order to test our apparatus measurements were carried out first at 90°K with neon. α_{exp} was measured as a function of pressure at different frequencies between 100 and 500 kHz. For the monoatomic gases the sound absorption is given by equation (1) which can be written as:

$$\alpha_{\mathrm{class}}/f = \frac{2\pi^2}{\gamma V}\left\{\frac{4}{3}\eta + \frac{\gamma - 1}{C_p}\lambda\right\} f/p. \qquad (6)$$

In fig. 9 α_{exp}/f is plotted as a function of f/p together with the theoretical

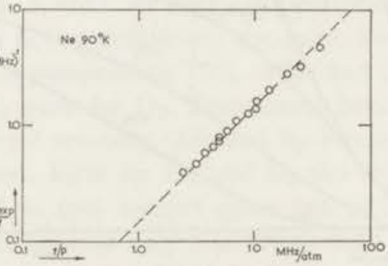

Fig. 9. α_{exp}/f as a function of f/p for neon at 90°K.
- - - - - theoretical curve ○ experimental points

TABLE I

Data necessary to calculate the classical sound absorption together with the calculated value of $\alpha_{\text{class}}p/f^2$ and $A = \dfrac{\Delta C'}{C_v(C_p - C')}$

gas	T °K	η μP	λ 10^{-6}cal cm^{-1} °K^{-1}s^{-1}	C'/R	C_v/R	C_p/R	C_p/C_v	V_0 m/s	$\alpha_{\text{class}}p/f^2$ cm^{-1} atm MHz^{-2}	A
nH_2	77.3	35.0	119	0.08	1.58	2.58	1.63	723	0.0125	0.0203
pH_2	77.3		126	0.30	1.80	2.80	1.56	708.0	0.0126	0.066
nD_2	77.3	48.2	109	1.04	2.54	3.54	1.39	472.0	0.0262	0.164
oD_2	77.3		118	1.43	2.93	3.93	1.34	464.0	0.0266	0.195
nH_2	90.2	39.7	138	0.155	1.655	2.655	1.60	774.6	0.0132	0.0376
pH_2	90.2		152	0.54	2.04	3.04	1.49	747.5	0.0135	0.106
nD_2	90.2	55.0	126	1.11	2.61	3.61	1.39	510.5	0.0276	0.170
oD_2	90.2		133	1.44	2.94	3.94	1.34	501.2	0.0280	0.196
HD	77.3	42.1	124	1.04	2.54	3.54	1.39	545.7	0.0197	0.164
HD	90.2	47.8	138	1.02	2.52	3.52	1.40	591.6	0.0205	0.162
nH_2	293	88.2	436	0.96	2.46	3.46	1.40	1306	0.0180	0.156
pH_2	293		459	1.09	2.59	3.59	1.39	1302	0.0180	0.168
nD_2	293	123	313	1.00	2.50	3.50	1.40	923.3	0.0355	0.160
oD_2	293		313	1.00	2.50	3.50	1.40	923.3	0.0355	0.160
HD	293	108	356	1.00	2.50	3.50	1.40	1066	0.0215	0.160
Ne	293	311	114	—	1.50	2.50	1.67	449	0.0200	
Ne	90	138	47.7	—	1.50	2.50	1.67	249	0.0146	

The data for the specific heat, the viscosity and the heat conductivity are taken from refs. 14, 18, 19 and 20. For neon the viscosity data are taken from ref. 21 and the heat conductivity, data from ref. 22.

straight line expected from equation (6). The viscosity, heat conductivity and specific heat data at 90°K, necessary to calculate the classical sound absorption in neon are given in table I. Good agreement was obtained between the experimental values and those calculated with equation (6) for the classical sound absorption, and measurements on the hydrogen isotopes were started. For n–H_2, p–H_2, n–D_2, o–D_2 and H_2 the absorption coefficient. α_{exp} was measured at 77 and 293°K as a function of $1/p$. Measurements were also performed for p–H_2 and o–D_2 at 90°K. From these measurements α_{exp}/f is obtained as a function of f/p. The value of α'/f, the excess-absorption coefficient divided by frequency, is than calculated by subtracting the calculated value of α_{class}/f from α_{exp}/f :

$$\alpha'/f = \alpha_{\text{exp}}/f - \alpha_{\text{class}}/f$$

TABLE II

Experimental results					
Sound absorption in n–H_2 at 293°K			Sound absorption in p–H_2 at 293°K		
f/p MHz/atm	α_{exp}/f (cm MHz)$^{-1}$	α'/f (cm MHz)$^{-1}$	f/p MHz/atm	α_{exp}/f (cm MHz)$^{-1}$	α'/f (cm MHz)$^{-1}$
0.690	0.270	0.258	1.53	0.483	0.455
0.928	0.307	0.290	2.51	0.734	0.68
0.850	0.300	0.285	3.84	1.05	0.98
1.48	0.491	0.464	2.73	0.82	0.77
2.49	0.778	0.733	3.89	1.13	1.06
4.72	1.49	1.40	6.65	1.44	1.32
1.50	0.532	0.505	7.16	1.74	1.61
3.68	1.13	1.06	10.6	2.04	1.85
5.25	1.46	1.36	21.1	2.46	2.08
12.1	2.21	1.99	16.0	2.30	2.01
8.52	2.19	2.04	29.4	2.34	1.81
20.7	2.14	1.96	29.5	2.43	1.90
15.6	2.30	2.02	52.3	2.43	1.49
24.9	2.02	1.61	41.6	2.45	1.70
39.3	2.06	1.36	57.3	2.51	1.48
51.9	2.11	1.18	94.8	2.88	1.17
72.1	2.42	1.12			
55.4	2.23	1.23			
89.7	2.74	1.13			

Sound absorption in n–D_2 at 293°K			Sound absorption in o–D_2 at 293°K		
f/p MHz/atm	α_{exp}/f (cm MHz)$^{-1}$	α'/f (cm MHz)$^{-1}$	f/p MHz/atm	α_{exp}/f (cm MHz)$^{-1}$	α'/f (cm MHz)$^{-1}$
0.633	0.293	0.270	0.974	0.478	0.433
1.10	0.463	0.424	1.32	0.660	0.613
1.60	0.657	0.600	1.93	0.862	0.793
1.60	0.709	0.652	3.25	1.43	1.31
2.90	1.21	1.11	6.32	2.18	1.96
5.67	2.18	1.98	4.57	1.69	1.52
4.07	1.64	1.50	6.35	2.32	2.11
6.47	2.30	2.07	8.80	2.63	2.32
9.03	2.67	2.35	15.4	3.32	2.77
11.1	2.90	2.50	22.4	3.37	2.57
8.43	2.53	2.33	16.8	3.14	2.50
14.7	3.14	2.62	25.2	3.20	2.31
19.5	3.20	2.51	36.4	3.34	2.05
23.9	3.38	2.54	43.4	3.34	1.80
31.5	3.31	2.19	61.9	3.34	1.14
60.0	3.64	1.51	51.2	3.44	1.62
45.8	3.49	1.86	83.3	4.04	1.25
86.6	4.54	1.47			

TABLE II (*Continued*)

Sound absorption in HD at 293°K		
f/p MHz/atm	α_{exp}/f (cm MHz)$^{-1}$	α'/f (cm MHz)$^{-1}$
3.33	0.225	0.153
5.05	0.298	0.189
7.26	0.432	0.276
13.8	0.864	0.567
9.75	0.572	0.362
12.6	0.718	0.447
20.6	1.25	0.81
30.5	1.78	1.12
22.8	1.25	0.76
28.7	1.64	1.02
41.2	2.18	1.29
53.0	2.80	1.66
67.6	3.41	1.96
89.5	3.91	1.99

Sound absorption in p–H_2 at 90°K			
f/p MHz/atm	α_{exp}/f (cm MHz)$^{-1}$	α'/f (cm MHz)$^{-1}$	$\alpha'\lambda\,(V_0/V)^2$
1.96	1.07	1.04	0.0777
2.75	1.37	1.33	0.0987
6.27	2.29	2.20	0.161
4.00	1.92	1.86	0.138
9.68	2.52	2.38	0.173
13.8	2.39	2.20	0.158
26.0	1.84	1.45	0.103
19.0	2.27	2.00	0.144
33.3	1.69	1.22	0.0867
49.9	1.57	0.86	0.0605
49.9	1.49	0.78	0.0553
69.2	1.49	0.50	0.0351

Sound absorption in o–D_2 at 90°K			
f/p MHz/atm	α_{exp}/f (cm MHz)$^{-1}$	α'/f (cm MHz)$^{-1}$	$\alpha'\lambda\,(V_0/V)^2$
1.55	0.93	0.89	0.045
2.19	1.20	1.12	0.056
2.96	1.60	1.52	0.076
5.24	3.20	3.06	0.152
7.94	3.70	3.48	0.172
12.2	5.32	4.98	0.245
25.3	6.93	6.12	0.290
18.3	6.69	6.14	0.296
30.9	6.91	6.04	0.283
51.1	6.06	4.53	0.207
82.4	5.79	3.48	0.158

Sound absorption in n–H_2 at 77°K		
f/p MHz/atm	α_{exp}/f (cm MHz)$^{-1}$	$\alpha' f$ (cm MHz)$^{-1}$
2.10	0.314	0.288
3.17	0.356	0.316
5.18	0.435	0.370
9.08	0.614	0.500
16.8	0.714	0.504
26.4	0.700	0.370
53.2	0.948	0.281

TABLE II (*Continued*)

Sound absorption in p–H_2 at 77°K

f/p MHz/atm	α_{exp}/f (cm MHz)$^{-1}$	α'/f (cm MHz)$^{-1}$	$\alpha'\lambda(V_0/V)^2$
1.03	0.499	0.487	0.0345
1.60	0.677	0.657	0.0464
2.56	0.972	0.940	0.0663
3.70	1.23	1.18	0.0828
4.86	1.46	1.40	0.0984
3.49	1.23	1.18	0.0828
5.28	1.51	1.44	0.101
6.28	1.57	1.49	0.104
7.93	1.68	1.58	0.110
12.00	1.61	1.41	0.098
8.42	1.69	1.58	0.110
14.7	1.57	1.38	0.0949
20.7	1.38	1.12	0.0772
42.9	1.25	0.71	0.0486

Sound absorption in o-D_2 at 77°K

f/p MHz/atm	α_{exp}/f (cm MHz)$^{-1}$	α'/f (cm MHz)$^{-1}$	$\alpha'\lambda\,(V_0/V)^2$
0.993	0.686	0.660	0.0306
1.19	0.875	0.843	0.391
1.70	1.25	1.20	0.0557
2.44	1.69	1.63	0.0756
3.80	2.63	2.53	0.117
5.80	3.65	3.50	0.161
9.86	5.63	5.37	0.245
7.04	4.74	4.55	0.204
12.2	6.62	6.29	0.284
21.6	6.31	5.73	0.262
16.4	6.41	5.97	0.266
23.7	6.26	5.63	0.247
20.7	7.58	7.03	0.310
27.6	7.08	6.35	0.277
33.3	7.07	6.18	0.266
50.2	7.11	5.77	0.244
41.7	7.00	5.89	0.251
41.7	6.90	5.79	0.247
52.9	6.14	6.00	0.254
74.5	6.25	4.27	0.180
35.5	8.62	7.68	0.330
57.8	5.96	4.43	0.187

Sound absorption in n–D_2 at 77°K

f/p MHz/atm	α_{exp}/f (cm MHz)$^{-1}$	α'/f (cm MHz)$^{-1}$
1.34	0.788	0.737
2.08	1.13	1.06
3.54	1.82	1.73
6.10	3.33	3.17
10.6	4.62	4.34
21.7	6.64	6.07
15.4	5.75	5.35
27.8	5.92	5.19
53.6	6.13	4.72
40.8	6.43	5.36
65.7	6.63	4.91
2.21	1.16	1.10
4.25	2.10	1.99
5.79	2.76	2.61
9.74	4.31	4.05
6.97	3.34	3.16
11.5	4.75	4.45
16.0	6.02	5.60
12.2	5.03	4.71
23.6	5.56	4.95
36.5	5.97	5.01
52.5	5.56	4.18
43.7	6.04	4.90
84.5	5.38	3.17

Sound absorption in HD at 77°K

f/p MHz/atm	α_{exp}/f (cm MHz)$^{-1}$	α'/f (cm MHz)$^{-1}$
3.16	0.230	0.168
4.80	0.237	0.142
8.29	0.320	0.157
14.4	0.550	0.229
28.1	0.980	0.426
20.1	0.664	0.270
30.5	1.07	0.470
64.1	2.06	0.800
84.0	2.83	1.18

(see for example Herzfeld and Litovitz[13]). α_{class}/f is calculated as a function of f/p with equation (6), using the data of the viscosity and the heat conductivity as given in table I. In table II and figs. 10–21 the experimental results of α'/f as a function of f/p are given. The experimental points in these figures have been connected by a solid line. As has been emphasized al-

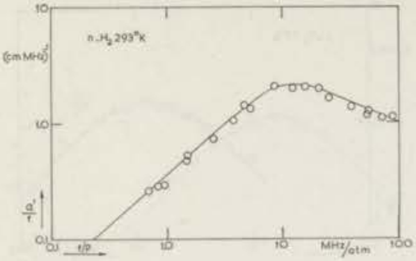

Fig. 10. α'/f as a function of f/p for n–H_2 at 293°K.

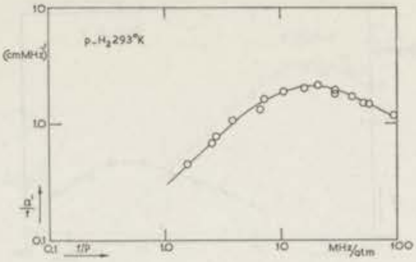

Fig. 11. α'/f as a function of f/p for p–H_2 at 293°K.

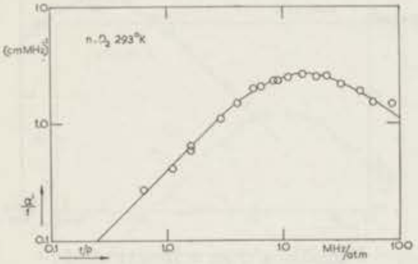

Fig. 12. α'/f as a function of f/p for n–D_2 at 293°K.

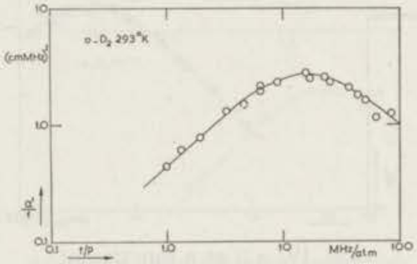

Fig. 13. α'/f as a function of f/p for o–D_2 at 293°K.

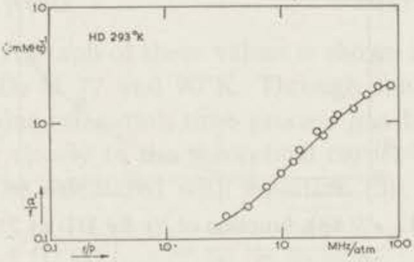

Fig. 14. α'/f as a function of f/p for HD at 293°K.

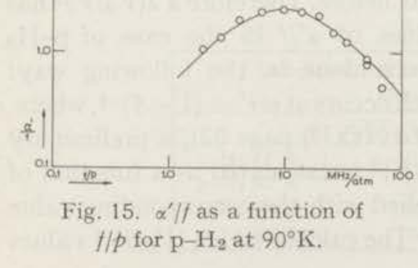

Fig. 15. α'/f as a function of f/p for p–H_2 at 90°K.

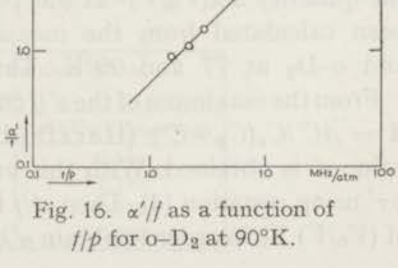

Fig. 16. α'/f as a function of f/p for o–D_2 at 90°K.

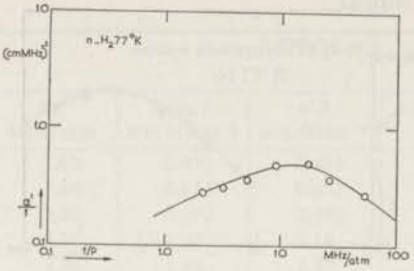

Fig. 17. α'/f as a function of f/p for n–H_2 at 77°K.

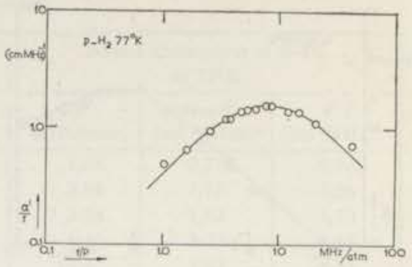

Fig. 18. α'/f as a function of f/p for p–H_2 at 77°K.

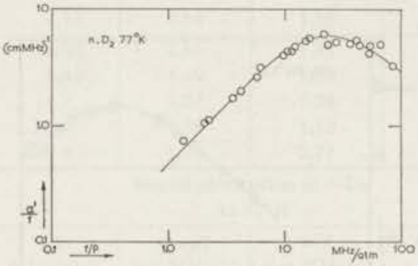

Fig. 19. α'/f as a function of f/p for n–D_2 at 77°K.

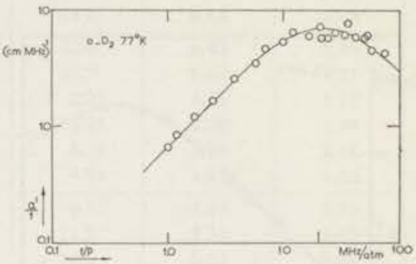

Fig. 20. α'/f as a function of f/p for o–D_2 at 77°K.

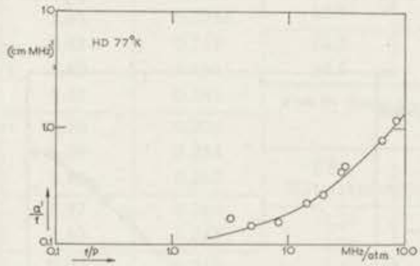

Fig. 21. α'/f as a function of f/p for HD at 77°K.

ready, reliable results can only be obtained from the measurements at low temperatures on p–H_2 and o–D_2 where a one-relaxation-time process is to be expected.

To analyze the measured absorption curves it is best suited to consider the quantity $\alpha'\lambda(V_0/V)^2$ as was pointed out before. Therefore $\alpha'\lambda(V_0/V)^2$ has been calculated from the measured values of α'/f in the case of p–H_2 and o–D_2 at 77 and 90°K. This has been done in the following way: From the maximum of the α'/f curve, which occurs at $\omega\tau' = (1-A)^{-\frac{1}{2}}$, where, $A = \Delta C'/C_v(C_p - C')$ (Herzfeld and Litovitz[13]) page 82), a preliminary value τ' is obtained. With this value $(V_0/V)^2$ is calculated as a function of $\omega\tau'$ using equation (4). Then α'/f is multiplied with the corresponding value of $(V_0/V)\ V_0$ in order to obtain $\alpha'\lambda(V_0/V)^2$. The calculated $\alpha'\lambda\ (V_0/V)^2$ values

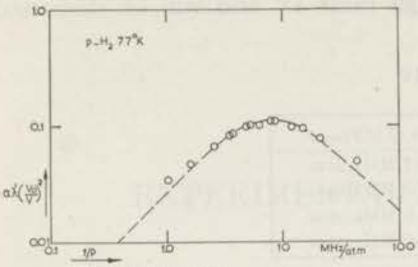

Fig. 22. $\alpha'\lambda(V_0/V)^2$ as a function of f/p for p–H_2 at 77°K.
- - - - - theoretical curve
○ experimental points.

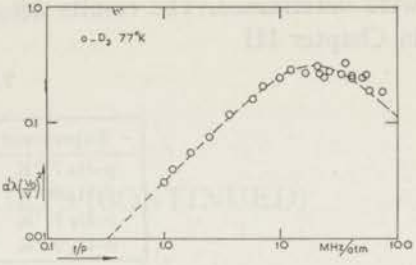

Fig. 23. $\alpha'\lambda(V_0/V)^2$ as a function of f/p for o–D_2 at 77°K.
- - - - - theoretical curve
○ experimental points.

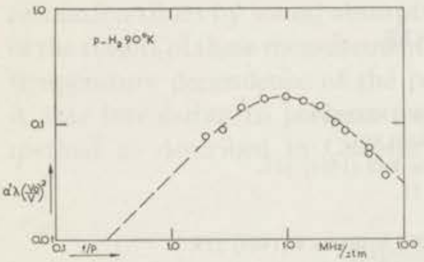

Fig. 24. $\alpha'\lambda(V_0/V)^2$ as a function of f/p for p–H_2 at 90°K.
- - - - - theoretical curve
○ experimental points.

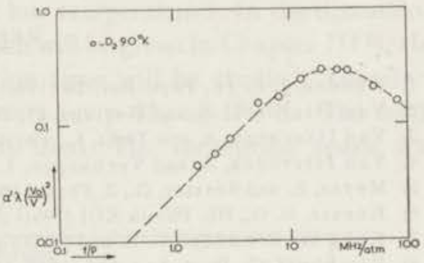

Fig. 25. $\alpha'\lambda(V_0/V)^2$ as a function of f/p for o–D_2 at 90°K.
- - - - - theoretical curve
○ experimental points.

are given in table II. A graph of these values is shown in figs. 22, 23, 24 and 25 for p–H_2 and o–D_2 at 77 and 90°K. Through the experimental points a dotted line for a one-relaxation-time process has been drawn. The experimental points fit closely to the theoretical curve. The height of the $\alpha'\lambda$ $(V_0/V)^2$ curves can be calculated with equation (3):

$$\alpha'\lambda\left(\frac{V_0}{V}\right)^2_{\max} = \frac{\pi}{2}\,\frac{\Delta C'}{C_v(C_p - C')}. \qquad (7)$$

The experimentally determined values of the maximum together with the values calculated from the specific-heat data are shown in table III. Agreement within a few percent is found.

From these $\alpha'\lambda$ $(V_0/V)^2$ curves the final, more accurate values of $(f/p)_{\max}$

TABLE III

Calculated and experimental maxima of the absorption curves		
	$\alpha'\lambda(V_0/V)^2_{\max}$(calc)	$\alpha'\lambda(V_0/V)^2_{\max}$(exp)
p–H_2 77°K	0.110	0.110
p–H_2 90°K	0.166	0.170
o–D_2 77°K	0.306	0.310
o–D_2 90°K	0.308	0.300

were determined. The results are given in table IV and will be discussed in Chapter III

TABLE IV

Experimental values of $(f/p)_{\max}$	
p–H_2 77°K	8.1 MHz/atm
p–H_2 90°K	9.3 MHz/atm
o–D_2 77°K	19.5 MHz/atm
o–D_2 90°K	23.0 MHz/atm

REFERENCES

1) Rhodes, J. E. Jr., Phys. Rev. **70** (1946) 932.
2) Van Itterbeek, A. and Mariens, P., Physica **4** (1937) 609.
3) Van Itterbeek, A. and Thijs, L., Physica **5** (1938) 889.
4) Van Itterbeek, A. and Verhaegen, L., Nature **167** (1951) 477.
5) Meyer, E. and Sessler, G., Z. Phys. **149** (1957) 15.
6) Kneser, H. O., Hb. Physik XI/I (1961) 170.
7) Kuhl, W., Schodder, G. R. and Schröder, F. K., Acustica **4** (1954) 519.
8) Kirchhoff, G., Pogg. Ann. **134** (1868) 177.
9) Stokes, G., Trans. Cambridge phil. Soc. **8** (1845) 287.
10) Keller, H. H., Phys. Z. **41** (1940) 386.
11) Greenspan, M., J. acoust Soc. America **22** (1950) 568; **28** (1956) 644.
12) Herzfeld, K. F. and Rice, R. O., Phys. Rev. **31** (1928) 691.
13) Herzfeld, K. F. and Litovitz, T. A., Absorption and dispersion of ultrasonic waves (Academic Press, New York and London, 1959).
14) Farkas, A., Orthohydrogen, Parahydrogen and Heavy Hydrogen (University Press, Cambridge, 1935).
15) Stewart, E. S. and Stewart, J. L., J. acoust. Soc. America **24** (1952) 194.
16) Geide, K., Acustica **13** (1963) 31.
17) Beyer, R. T., J. acoust. Soc. America **29** (1957) 243.
18) Woolley, H. W., Scott, R. B. and Brickwedde, F. G., J. Res. Nat. Bur. Stand. **4** (1948) 379.
19) Coremans, J. M. J., Van Itterbeek, A., Beenakker, J. J. M., Knaap, H. F. P. and Zandbergen, P., Commun. Kamerlingh Onnes Lab., Leiden No. 311*a* and 312*d*; Physica **24** (1958) 557 and 1102.
20) Ubbink, J. B., Commun. Leiden No. 273*b*; Physica **14** (1948) 165.
21) Trautz, M. and Binkele, H. E., Ann. Phys. (Leipzig) **5** (1930) 561.
22) Weber S., Comm. Phys. Lab. Leiden, Suppl. No. 42*b*.

CHAPTER II

EXPERIMENTAL RESULTS (CONTINUED)

1. *Sound absorption measurements in para hydrogen at 170°K.* Measurements were reported in a Chapter I 1), on the determination of rotational relaxation times by sound absorption at low temperatures. In the discussion of the results of these measurements, which will be given in Chapter III 2), the temperature dependence of the relaxation time will be studied. Therefore it was interesting to perform experiments on p–H_2 at 170°K. The same method as described in Chapter I was used. The measuring space was

TABLE I

Experimental results
Sound absorption in p–H_2 at 170°K

f MHz	f/p MHz/atm	α_{exp}/f (cm MHz)$^{-1}$	α'/f (cm MHz)$^{-1}$	$\alpha'\lambda(V_0/V)^2$
0.533^4	0.98^3	0.478	0.461	0.045
	1.21	0.634	0.613	0.060
	1.76	0.900	0.870	0.084
	2.35	1.14^9	1.10^8	0.107
	3.59	1.73^1	1.66^9	0.161
0.337^1	2.54	1.29^1	1.14^7	0.111
	3.83	1.87^2	1.80^6	0.174
0.533^4	5.42	2.41	2.32	0.222
	9.06	3.31	3.15	0.297
0.377^1	6.40	2.66	2.55	0.243
	11.29	3.47	3.27	0.305
0.533^4	15.97	3.72	3.44	0.315
0.287^2	8.60	3.42	3.27	0.309
	11.63	3.54	3.34	0.311
0.533^4	21.6	3.60	3.23	0.291
0.377^1	15.3	3.60	3.34	0.307
0.245^7	9.95	3.59	3.42	0.321
	16.94	3.82	3.53	0.319
0.377^1	26.0	3.33	2.88	0.257
0.533^4	36.8	2.89	2.25	0.199
0.287^2	19.8	3.70	2.36	0.304
	33.3	3.13	2.55	0.226
0.377^1	43.7	2.95	2.19	0.193
0.245^7	28.5	3.40	2.91	0.259
	50.6	2.72	1.85	0.162
	81.1	2.56	1.16	0.101
	134.3	2.73	0.41	0.036

surrounded by a bath of ethylene in order to obtain a temperature of 170°K. The temperature was determined from the bath pressure and from the resistance of a Pt-thermometer mounted inside the measuring space. Agreement to within 0.1°K was found.

In table I the results for α_{exp}/f and α'/f are given. α'/f is again obtained by subtracting from α_{exp}/f the calculated value of α_{class}/f. The data necessary to calculate α_{class} are given in table II. From the α'/f values $\alpha'\lambda(V_0/V)^2$ was calculated as indicated in Chapter I. The results are given in table I. The values of α'/f and $\alpha'\lambda(V_0/V)^2$ are given as functions of f/p in figs. 1 and 2. As could be expected from the occupation of the rotational levels (see fig. 7 Chapter I) the $\alpha'\lambda(V_0/V)^2$ points fit the theoretical curve for a one-relaxation-time process. This curve is shown by a dotted line in

TABLE II

Data necessary to calculate the classical sound absorption together with the calculated value of $\alpha_{class}\, p/f^2$ and $A = \dfrac{\Delta C'}{C_v\,(C_p - C')}$

gas	T °K	η μP	λ 10^{-6} cal cm^{-1} °K^{-1} s^{-1}	C'/R	C_v/R	C_p/R	C_p/C_v	V_0 m/s	$\alpha_{class}\, p/f^2$ cm^{-1} atm MHz^{-2}	A
p–H_2	170	61	271	1.47	2.97	3.97	1.34	972	0.0173	0.198

These data for the specific heat are taken from ref. 3.
The viscosity and heat conductivity data are taken from ref. 4

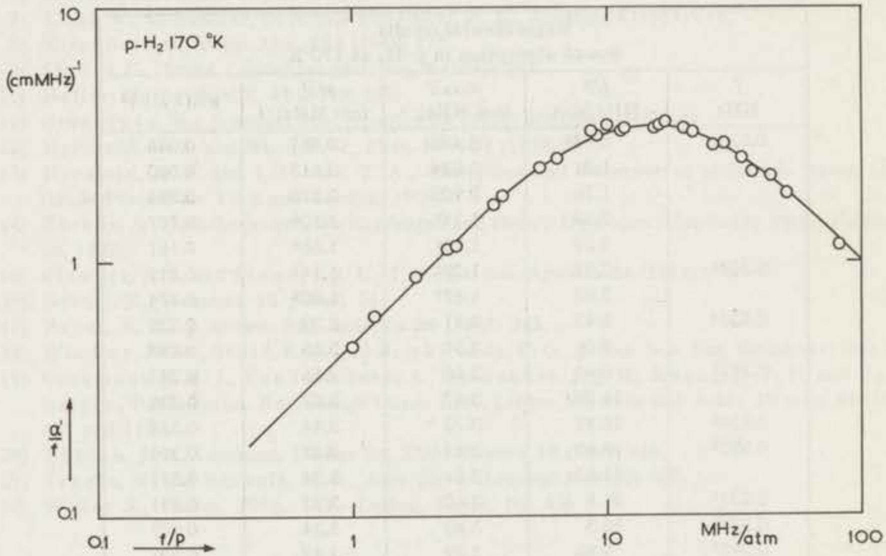

Fig. 1. α'/f as a function of f/p for p–H_2 at 170°K.
○ experimental points.

fig. 2. Thus the $(f/p)_{\max}$ value could be determined in the usual way. The theoretical value of the maximum of the $\alpha'\lambda(V_0/V)^2$ curve, calculated with eq. (7) Chapter I from the rotational specific heat, is 0.311. The experimental value of 0.320 is in good agreement with this value. The result is

$$(f/p)_{\max} = 13.5 \text{ MHz/atm for p–H}_2 \text{ at } 170°\text{K}.$$

This result will be discussed in Chapter III together with the results reported in Chapter I.

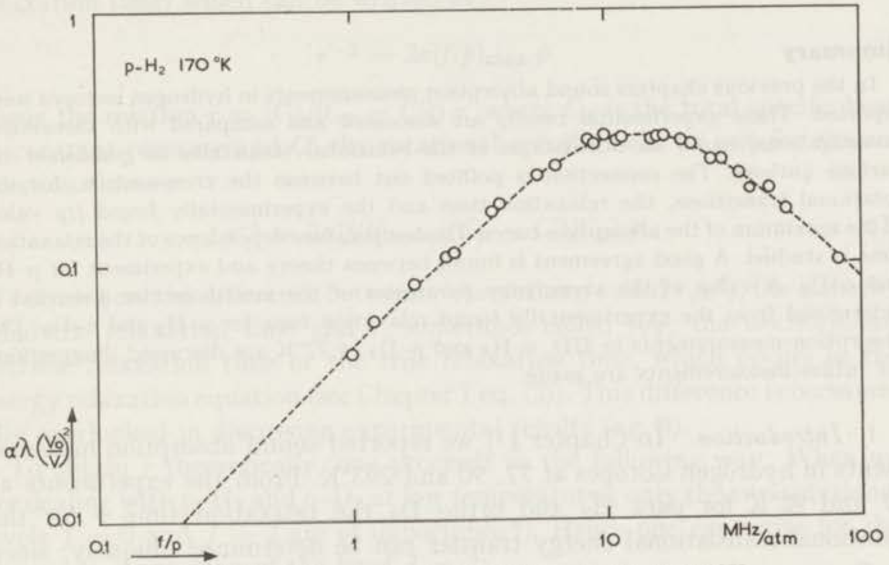

Fig. 2. $\alpha'\lambda(V_0/V)^2$ as a function of f/p for p–H_2 at 170°K.
— — — theoretical curve.
○ experimental points.

REFERENCES

1) Sluijter, C. G., Knaap, H. F. P. and Beenakker, J. J. M., Commun. Kamerlingh Onnes Lab. Leiden No. 337*c*; Physica **30** (1964) 745.

2) Sluijter, C. G., Knaap, H. F. P. and Beenakker, J. J. M., Commun. Supl. No. 123*a*; Physica to be published.

3) Farkas, A., Orthohydrogen, Parahydrogen and Heavy Hydrogen (University Press, Cambridge, 1935).

4) Woolley, H. W., Scott, R. B. and Brickwedde, F. G., J. Res. Nat. Bur. Stand. **4** (1948) 379.

Chapter III

CALCULATION OF THE RELAXATION TIME FROM THE COLLISION CROSS-SECTION AND COMPARISON WITH THE EXPERIMENTAL RESULTS

Summary

In the previous chapters sound absorption measurements in hydrogen isotopes were reported. These experimental results are discussed and compared with theoretical investigations, based on calculations of the rotational transitions as published by various authors. The connection is pointed out between the cross-section, for the rotational transitions, the relaxation time and the experimentally found f/p value of the maximum of the absorption curve. The temperature dependence of the relaxation time is studied. A good agreement is found between theory and experiment for p–H_2 and o–D_2. A value of the asymmetry parameter of the intermolecular potential is determined from the experimentally found relaxation time for p–H_2 and o–D_2. The absorption measurements in HD, n–H_2 and n–D_2 at 77°K are discussed. Suggestions for future measurements are made.

1. *Introduction.* In Chapter I[1]) we reported sound absorption measurements in hydrogen isotopes at 77, 90 and 293°K. From the experiments at 77 and 90°K for para H_2 and ortho D_2 the relaxation time τ for the rotational-translational energy transfer can be determined uniquely, since in these cases one deals with a single relaxation time process. The same is true for the sound absorption measurements in para H_2 at 170°K which are reported in Chapter II[2]). To discuss our experimental results we will first point out the connection between the rotational relaxation time and the transition cross-section as calculated from the intermolecular potential. The theoretical results of several authors will be used. As no direct values of the relaxation time as function of temperatures are given by these authors we will indicate how one can derive these values from their numerical data on the rotational transition cross-sections, given as a function of the incident energy of the incoming particle. For some systems, which have two relaxation times, the absorption curve can be calculated using the experimental- and theoretical results on systems with one relaxation time. This will be done to analyze the experimental results on n–H_2 and n–D_2 at 77°K, as reported in Chapter I. Also the experimental results of other authors will be discussed. Suggestions will be given for future experiments.

2. *Connection between relaxation time and collision cross-section.* From the experimental results for the absorption coefficient in the case of a system with one relaxation time one can determine the value of $(f/p)_{\max}$ *i.e.* the ratio of frequency f and pressure p, at which the $\alpha'\lambda(V_0/V)^2$ curve passes through its maximum. Here α' is the excess sound absorption due to relaxation as defined in Chapter I, λ the wavelength, V the velocity and V_0 the velocity at zero frequency of the sound wave. As follows from eq. (3) of Chapter I this maximum is reached for $\omega\tau' = 1$ ($\omega = 2\pi f$ and τ' is a relaxation time) which can be written as:

$$\tau'^{-1} = 2\pi(f/p)_{\max}\, p. \tag{1}$$

Using the relation $\tau = (C_p/(C_p - C'))\,\tau'$ where C_p is the total specific heat at constant pressure and C' the rotational specific heat we get for the relaxation time τ:

$$\tau^{-1} = 2\pi(f/p)_{\max}\,((C_p - C')/C_p)\, p. \tag{2}$$

We stress here the difference between τ', sometimes called τ_{pS}[3], the isobaric-adiabatic relaxation time and τ, sometimes called τ_{VT}, the isochoric-isothermic relaxation time or the true relaxation time, which occurs in the energy relaxation equation (see Chapter I eq. (2)). This difference is occasionally overlooked in discussing experimental results (*e.g.*[4]).

To obtain τ theoretically, one proceeds in the following way: When we are dealing with p–H_2 and o–D_2 at low temperatures, only the two rotational levels $J = 0$ and $J = 2$ are of importance[*]. Hence one can write for the change in occupation of the level $J = 2$:

$$-\frac{\mathrm{d}n_2}{\mathrm{d}t} = n_2 f_{20} - n_0 f_{02} \tag{3}$$

where n_0 and n_2 denote the numbers of molecules in the state $J = 0$ and $J = 2$ respectively, while f_{02} is the transition probability for a molecule to go from a state with $J = 0$ to a state with $J = 2$ and f_{20} the probability to go from $J = 2$ to $J = 0$. Using the equilibrium condition:

$$0 = -\frac{\mathrm{d}n_2}{\mathrm{d}t} = n_2^0 f_{20} - n_0^0 f_{02} \tag{4}$$

where the superscript refers to the equilibrium state, one gets for eq. (3):

$$-\frac{\mathrm{d}n_2}{\mathrm{d}t} = (n_2 - n_2^0)(f_{20} + f_{02}). \tag{5}$$

---

[*] Instead of $J = 0$ and $J = 2$ one can read in the following $J = i$ and $J = j$ if one wants to consider the transition from the i^{th} to the j^{th} level.

If we denote the energy gap between the state with $J = 0$ and $J = 2$ by ε, the internal energy of the system is given by $E' = n_2\varepsilon$.

Multiplication of equation (5) with ε results in:

$$-\frac{\mathrm{d}E'}{\mathrm{d}t} = [E' - E'(T_{\mathrm{tr}})](f_{20} + f_{02}) \tag{6}$$

where $E(T_{\mathrm{tr}}) = n_2^0\varepsilon$ is the value of the internal energy E' in equilibrium with the translational degrees of freedom at temperature T_{tr}. This equation has the same form as the relaxation equation for the internal energy (Chapter I eq. (2)). It can be used to express the relaxation time in terms of f_{02} and f_{20}:

$$\tau^{-1} = f_{20} + f_{02}. \tag{7}$$

As a result of the condition of statistical equilibrium one has:

$$f_{20} = f_{02}(g_0/g_2)\exp(\varepsilon/\kappa T). \tag{8}$$

Here κ is Boltmann's constant and T the absolute temperature, g_0 and g_2 are the statistical weights of rotational levels $J = 0$ and $J = 2$. The statistical weight of the J^{th} rotational level is $2J + 1$. Assuming transitions between rotational-energy states occur at collisions only, one has in the limit of low pressures:

$$f_{02} = \left(\frac{8}{\pi\mu\kappa T}\right)^{\frac{1}{2}} p\langle Q_{02}\rangle_T. \tag{9}$$

The terms on the right have the following meaning: $(8/\pi\mu\kappa T)^{\frac{1}{2}}\, p$ represents the number of molecules hitting unit area per second at temperature T and $\langle Q_{02}\rangle_T$ is the averaged inelastic cross-section for the $0 \to 2$ transition at that temperature (see e.g. ref. 5). $\langle Q_{02}\rangle_T$ is obtained by averaging $Q(k)$, the inelastic scattering cross-section for incident wave number k, over the Maxwellian distribution of the incident numbers k at temperature T.

This inelastic collision cross-section $Q(k)$ has been calculated as a function of the wave numbers k of the incident particle by various authors for different angle-dependent intermoleculair potentials, $V(R, \chi)$. Instead of considering the relaxation time τ it is however sometimes more useful to consider a number Z, which is of the order of the number of collisions necessary for energy transfer. This number Z is obtained by dividing τ by τ_c, the average time between two collisions.

The following scheme indicates the different steps that are taken in deriving theoretically the relaxation time τ and collision number Z:

$$V(R, \chi) \to Q_{02}(k) \to \langle Q_{02}\rangle_T \to f_{02}(T) \to \tau(T) \to Z(T). \tag{10}$$

Starting from the experimental results the following steps are required to obtain τ and Z:

$$(f/p)_{\max} \to \tau' \to \tau \to Z. \tag{11}$$

The most complicated step is the calculation of $Q(k)$ from the intermolecular potential $V(R, \chi)$. To obtain $\langle Q_{02}\rangle_T$ one must integrate $Q(k)$ over the Maxwellian distribution of the wave numbers k. We will discuss a simple method to approximate this integration.

3. *The inelastic scattering cross-section* $Q(k)$. The general solution of the collision problem of two rigid rotators is rather complicated. Hence most authors treat the problem of two colliding molecules (as *e.g.* H_2 and D_2) as a collision between a sphere and a rigid rotator with internal degrees of freedom (see *e.g.* ref. 6). In this model simultaneous transitions in both molecules are not considered. Rather complete calculations for the hydrogen isotopes were performed by Takayanagi[7]). Davison[8]) published more rigorous calculations on para hydrogen, Roberts[9]) treated both hydrogen-hydrogen and hydrogen-helium collisions. Recently Takayanagi published a comprehensive discussion[10]) of his own work and that of Davison[8]) and Roberts[9]).

We will first discuss the work of Takayanagi[7]). He used the distorted wave approximation to solve the set of coupled differential equations arising from the Schrödinger equation of the collision problem. A further approximation was introduced[4]) to solve the radial part of the Schrödinger equation:

$$\left\{\frac{\mathrm{d}^2}{\mathrm{d}R^2} + k^2 - \frac{J(J+1)}{R^2} + V(R, \chi)\right\}\varphi(R) = 0. \tag{12}$$

Here k is the incident wave number, R the distance between the two molecules, J the rotational quantum number, $V(R, \chi)$ the intermolecular potential and $\varphi(R)$ the radial wave function. At distances that are of importance for the transition (*i.e.* around the classical turning point), the quantity $J(J+1)/R^2$ may be considered constant for small J values, as compared to the repulsive potential at this point.

Takayanagi therefore replaced:

$$k^2 - \frac{J(J+1)}{R^2} \text{ by } \bar{k}^2 = k^2 - \frac{J(J+1)}{R_c^2}$$

in which $\bar{k}$ is called the modified wave number. The value of the constant R_c in this approximation is somewhat arbitrary but is of the order of the classical distance of closest approach. For mathematical convenience Takayanagi used a potential of the Morse-type:

$$V(R, \chi) = A \exp\{-2\alpha(R - R_0)\} - 2A \exp\{-\alpha(R - R_0)\} + \\ + \beta A \exp\{-2\alpha(R - R_0)\} P_2(\cos\chi) \tag{13}$$

where $P_2(\cos\chi)$ is the second Legendre polynomial, A, R_0 and α are constants with the following values $A = 1.1 \times 10^{-4}$, $R_0 = 6.4$, $\alpha = 0.935$ all expressed in atomic units*).

The meaning of χ and R are illustrated in fig. 1. As mentioned before, one of the colliding molecules is considered spherical, hence only one angle enters in the problem. Eq. (13) is a spherical Morse-type potential with an angle-dependent repulsive part, the strength of which is determined by the adjustable parameter β.

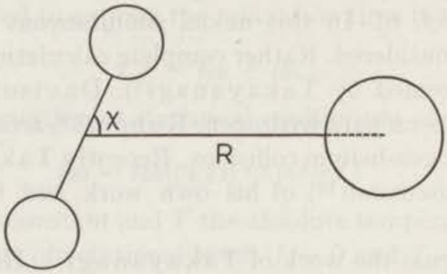

Fig. 1. The colliding molecules according to Takayanagi.

Takayanagi calculated the rotational transition cross-sections for the 0 → 2, 1 → 3 and 2 → 4 transition in H_2 and D_2, and for the 0 → 1 and 1 → 2 transition in HD. The parameters β and R_c appear in his results on hydrogen and deuterium only in an external factor $\beta^2 R_c^2$. This is not true for HD because the potential departs from the form of eq. (13) since the centre of gravity of the HD molecule does not coincide with its geometrical midpoint.

He obtained the following expression for $\langle Q_{02} \rangle_T$:

$$\langle Q_{02} \rangle_T = \pi R_c^2 \beta^2 \int_0^\infty M(\bar{k}) \frac{F_0(\bar{k})}{\beta^2} \mathrm{d}\bar{k} \tag{14}$$

where

$$F_0(\bar{k}) = \frac{Q(\bar{k})}{\pi R_c^2}$$

and $M(\bar{k})$ is the distribution of the modified wave numbers in one direction:

$$M(\bar{k}) = \frac{\bar{k}}{\mu\kappa T} \exp(-\bar{k}^2/2\mu\kappa T). \tag{15}$$

---

*) In these calculations atomic units are used. Here the unit of length is chosen equal to the radius a_0 of the first Bohr orbit, the value in c.g.s. units being $(0.5282 \pm 0.0004) \times 10^{-8}$ cm. The unit of mass is the mass of the electron in c.g.s. units $(9.035 \pm 0.010)\ 10^{-28}$ g. The unit of time is the time for an electron to go $(2\pi)^{-1}$ revolutions in the first Bohr orbit (in c.g.s. units 2.419×10^{-17} s).

This system of atomic units is discussed by Condon and Shortley[11]). The values of the basic units in the c.g.s. system are taken from this work. The atomic units have the advantage of avoiding the use of large powers of ten in the calculations. In this system Planck's constant h is equal to 2π which is convenient for theoretical purposes.

TABLE I

Transition probabilities per collision as calculated by Takayanagi 7)

$F_0(\tilde{k})/\beta^2$				$F_0(\tilde{k})$	
$\tilde{k}^2$	$H_2(0 \to 2)$	$D_2(0 \to 2)$	$D_2(1 \to 3)$	$\tilde{k}^2$	$HD(0 \to 1)$
6.35	0.305	0.569	—	3.50	0.175
6.86	0.409	0.747	—	5.47	0.257
7.84	0.655	1.070	—	7.87	0.341
9.24	1.008	1.517	—	10.71	0.420
10.69	1.41	1.98	0.142	13.99	0.491
12.29	—	—	0.281	17.71	0.553
13.99	2.31	3.06	0.455	21.86	0.608
14.69	—	—	—	26.45	0.654
15.79	—	—	0.662	31.50	0.694
17.72	3.34	4.22	0.913	36.94	0.728
21.81	4.49	5.49	1.48	—	—
26.42	5.75	6.87	2.14	—	—
31.47	7.12	8.34	2.91	—	—
36.97	8.59	9.92	3.76	—	—
42.77	10.16	11.60	4.69	—	—
49.14	11.83	13.4	5.69	—	—
55.95	13.7	15.2	6.77	—	—
63.20	15.5	17.2	7.91	—	—
70.73	17.5	19.3	9.12	—	—
78.85	19.5	21.5	10.40	—	—
87.42	21.8	23.9	—	—	—
	$\tilde{k}_0^2 = 6.10$	$\tilde{k}_0^2 = 6.10$	$\tilde{k}_0^2 = 10.16$		$\tilde{k}_0^2 = 2.29$
T °K	$\bar{F}_0/\beta^2$	$\bar{F}_0/\beta^2$	$\bar{F}_0/\beta^2$	T °K	$\bar{F}_0$
100	2.65×10^{-3}	8.99×10^{-2}	4.02×10^{-3}	—	—
200	5.91×10^{-2}	5.36×10^{-1}	6.77×10^{-2}	200	0.127
300	1.96×10^{-1}	1.13	2.12×10^{-1}	—	—

The wave numbers are expressed in atomic units.
$\bar{F}_0/\beta^2 = \langle Q \rangle_T / \pi R_c^2 \beta^2$.

He tabulated $F_0(\bar{k})/\beta^2$ as a function of $\bar{k}$. The results for H_2 and D_2 are shown in table I. In the case of HD where β cannot be used as an adjustable parameter $F_0(\bar{k})$ is given in table I as function of $\bar{k}^2$ for a value of $\beta = 0.075$.

Davison[8]) performed a more complete calculation on p–H_2. He used the full distorted wave method, without the modified wave number approximation. This made extensive machine calculations necessary. Furthermore he overcame the mathematical difficulties involved in treating both particles as non-spherical. He performed his calculations for two potentials.

a) A Morse-type potential, which now contains two angle dependent terms:

$$V(R, \chi) = A \exp\{-2\alpha(R - R_0)\} - 2A \exp\{-\alpha(R - R_0)\} + \beta A \exp\{-2\alpha(R - R_0)\}\{P_2(\cos \chi_1) + P_2(\cos \chi_2)\}. \tag{16}$$

The constants A, R_0 and α are the same as those used by Takayanagi, *i.e.* $A = 1.1\ 10^{-4}$, $R_0 = 6.4$, $\alpha = 0.935$, β is again an adjustable parameter. For the meaning of R, χ_1, χ_2 see fig. 2.

b) An exponential-six potential, which again contains two angle dependent terms, and in which also the non-sphericity of the long-range forces is taken into account:

$$V(R,\chi) = A\exp\{-2\alpha(R-R_0)\} - BR^{-6} + [\beta A\exp\{-2\alpha(R-R_0)\} - \\ - DR^{-6}]\,[P_2(\cos\chi_1) + P_2(\cos\chi_2)]. \qquad (17)$$

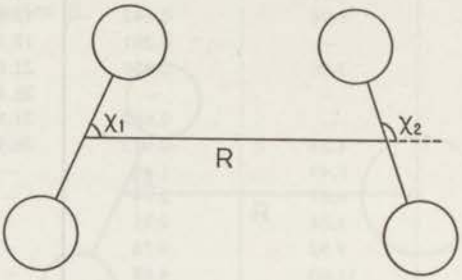

Fig. 2. The colliding molecules according to Davison.

A, R_0 and α have the values mentioned above, while B and D are given by $B = 11.0$, $D = 0.8$ (atomic units). His results can be expressed by:

$$\langle Q_{02}\rangle_T = \int_0^\infty M(k)\,Q(k)\,\mathrm{d}k \qquad (18)$$

where $M(k)$ is the normal Maxwellian distribution of the incident wave numbers in all directions at temperature T:

$$M(k) = \frac{k^3}{2(\mu\kappa T)^2}\exp(-k^2/2\mu\kappa T). \qquad (19)$$

In the case of the Morse potential Davison obtained cross-sections proportional to β^2. So again β can be used as an external parameter (Davison actually uses $\beta = 0.075$). This is opposed to his results for the exponential potential, where the parameters β and D have the fixed values of 0.14 and 0.8 respectively. His results are represented in table II. Note that β in the exp -6 potential has not the same meaning as in the Morse potential, owing to the different form of the non-spherical part of the potential.

Finally Roberts[9]) calculated the transition cross-section for two cases: collisions between hydrogen and hydrogen and between helium and hydrogen. He used essentially the same method as Davison, taking a Morse potential for the interaction. As already stated by Roberts himself his results on hydrogen are in good agreement with those of Davison[8]). These results are shown in table III. The He–H_2 cross-sections are much larger than the H_2–H_2 cross-sections (see fig. 3).

TABLE II

Cross-sections for the 0 → 2 rotational transition in H_2 as calculated by Davison 8)

k^2	$Q_{02}(k)$ Morse $\beta = 0.075$	$Q_{02}(k)$ exp.-six $\beta = 0.14$
5.95	0.0000	0.0000
6.76	0.0362	0.0551
7.84	0.0775	0.1335
9.61	0.1508	0.2964
12.25	0.2713	0.5831
16.25	0.4416	1.0146
25.00	0.8118	2.0416
39.06	—	3.5324
T °K	$\langle Q_{02}\rangle_T$	
197.1	3.3×10^{-2}	6.8×10^{-2}
298.4	—	2.2×10^{-1}

The cross-sections and wave numbers are expressed in atomic units

TABLE III

Cross-sections for the 0 → 2 rotational transition in H_2 as calculated by Roberts 9)

E_{inc} eV	k^2	$Q_{02}(k)$ $\beta = 0.075$
0.05	6.791	0.0263
0.06	8.149	0.0710
0.07124	9.676	0.1305
0.08	10.87	0.1803
0.09	12.22	0.2391
0.10	13.58	0.2979
0.15	20.37	0.5821
0.20	27.16	0.8398
0.25	33.96	1.075

The cross-sections and wave numbers are expressed in atomic units

4. *Calculation of τ and Z from the numerical $Q(k)$ data.* Following scheme (10) τ or Z can be calculated from the numerical $Q(k)$ values, taking care that when using the data of Davison we have to take eq. (19) to average over the Maxwellian distribution, while when using the data of Takayanagi we have to take eq. (15).

First let us make a general remark about this calculation. Since:

$$Q(k) = 0 \quad \text{if} \quad k < k_0 \quad \text{and}$$
$$F_0(k) = 0 \quad \text{if} \quad k < k_0$$

where $k_0^2 = 2\mu\varepsilon$ and $\bar{k}_0^2 = 2\mu\varepsilon$, the region below k_0 or $\bar{k}_0$ gives no contribution to the integral in the averaging process. Hence we can write for the integration following Davison:

$$\langle Q_{02}\rangle_T = \int\limits_{k_0}^{\infty} \frac{k^3}{2(\mu\kappa T)^2} \exp\left(-\frac{k^2}{2\mu\kappa T}\right) Q(k)\,\mathrm{d}k. \tag{20}$$

This may be transformed by substituting $K = k^2 - k_0^2$:

$$\langle Q_{02}\rangle_T = \exp(-k_0^2/2\mu\kappa T) \int\limits_0^{\infty} \frac{K + k_0^2}{4(\mu\kappa T)^2} \exp(-K/2\mu\kappa T)\, Q'(K)\,\mathrm{d}K \tag{21}$$

where $Q'(K)$ is $Q(k)$ expressed as a function of K.
or:

$$\langle Q_{02}\rangle_T = \exp(-k_0^2/2\mu\kappa T)\, \mathrm{I}_{\mathrm{Da}}(T) \tag{22}$$

where I_{Da} stands for the integral over K.

Following Takayanagi one writes:

$$\langle Q_{02}\rangle_T = \pi R_c^2\beta^2 \int\limits_{k_0}^{\infty} \frac{\bar{k}}{\mu\kappa T} \exp\left(\frac{-\bar{k}^2}{2\mu\kappa T}\right) \frac{F_0(\bar{k})}{\beta^2}\,\mathrm{d}\bar{k} \tag{23}$$

or, by substituting $\tilde{K} = \bar{k}^2 - \bar{k}_0^2$,
one obtains:

$$\langle Q_{02}\rangle_T = \pi R_c^2\beta^2 \exp(-\bar{k}_0^2/2\mu\kappa T) \int\limits_0^{\infty} \frac{\exp\,(-\tilde{K}/2\mu\kappa T)}{2\mu\kappa T}\, \frac{F_0'(\tilde{K})}{\beta^2}\,\mathrm{d}\tilde{K} \tag{24}$$

where $F_0'(\tilde{K})$ is $F_0(\bar{k})$ expressed as function of $\tilde{K}$
or:

$$\langle Q_{02}\rangle_T = \pi R_c^2\beta^2 \exp(-\bar{k}_0^2/2\mu\kappa T)\, I_{\mathrm{Ta}}(T) \tag{25}$$

where I_{Ta} stands for the integral over K
or for both cases:

$$\langle Q_{02}\rangle_T = \exp(-\varepsilon/\kappa T)\, I(T) \tag{26}$$

where $I(T)$ stands for $I_{\mathrm{Da}}(T)$ or $R_c^2\beta^2 I_{\mathrm{Ta}}(T)$ respectively. In our calculation we will always take $R_c = 6.4$ (a.u.). It turns out that $Q'(K)$ or $F'(\tilde{K})/\beta^2$ can be approximated by simple polynomials of K or $\tilde{K}$. This makes it possible to approximate the integral by an analytic integration. This will be discussed in detail below. Using equation (26) for $\langle Q\rangle_T$ together with equations (7), (8) and (9), we got the following equation for the relaxation time:

$$\tau^{-1} = a_0^2\left(\frac{8}{\pi\mu\kappa T}\right)^{\frac{1}{2}} p(g_0/g_2 + (\exp(-\varepsilon/\kappa T))\, I(T). \tag{27}$$

The factor a_0^2 occurs because $I(T)$ is expressed in atomic units. To calculate $Z = \tau/\tau_c$ we define first the time τ_c between collisions by the expression:

$$\tau_c = \Lambda/\overline{W}. \tag{28}$$

Here $\overline{W}$ is the average thermal velocity of the molecules:

$$\overline{W} = (8\kappa T/2\pi\mu)^{\frac{1}{2}}, \tag{29}$$

Λ is the mean free path of the molecules treated as hard spheres with diameter σ:

$$\Lambda^{-1} = \sqrt{2}n\pi\sigma^2 \tag{30}$$

and n is here the particle density of the molecules *i.e.* $n = p/\kappa T$. In this way we obtain:

$$\tau_c^{-1} = \pi\sigma^2\left(\frac{8}{\pi\mu\kappa T}\right)^{\frac{1}{2}} p. \tag{31}$$

For σ we will use the value 2.93 Å (cf. ref. 12).

From eqs (27) and (31) we get:

$$Z^{-1} = \frac{a_0^2}{\pi\sigma^2}\,(g_0/g_2 + (\exp -\varepsilon/\kappa T))\,I(T). \tag{32}$$

We will first discuss the way in which the integral $I(T)$ was calculated in the various cases, namely:

a. Davison, Morse potential, eq. (16) H_2 (0 → 2) Da 1
b. Davison, exponential-six potential, eq. (17) H_2 (0 → 2) Da 2
c. Takayanagi, Morse potential, eq. (13) H_2 (0 → 2) Ta
d. Takayanagi, Morse potential, eq. (13) D_2 (0 → 2) Ta
e. Takayanagi, modified Morse potential, eq. (39) HD (0 → 1) Ta
f. Roberts, Morse potential, eq. (13) H_2 (0 → 2) Ro

In these calculations atomic units are used throughout.

a. Davison, Morse potential H_2 (0 → 2). In fig. 3 the values of $Q(k)$ are plotted as function of k^2. (These values are given in table II.) As this results in a straight line, we approximated these values by the equation:

$$Q(k) = c(k^2 - k_0^2), \text{ where } k_0^2 = 6 \text{ and } c = 0.043.\ (\beta = 0.075). \tag{33}$$

Using this approximation when we perform the integration (eqs. (21), (22)) analytically, we obtain:

$$I_{\mathrm{Da}}(T) = 4c\mu\kappa T\left(1 + \tfrac{1}{2}\,\frac{k_0^2}{2\mu\kappa T}\right). \tag{34}$$

b. Davison, exponential-six potential H_2 (0 → 2). To integrate the value of $Q(k)$ derived for the exponential-six potential as given in table

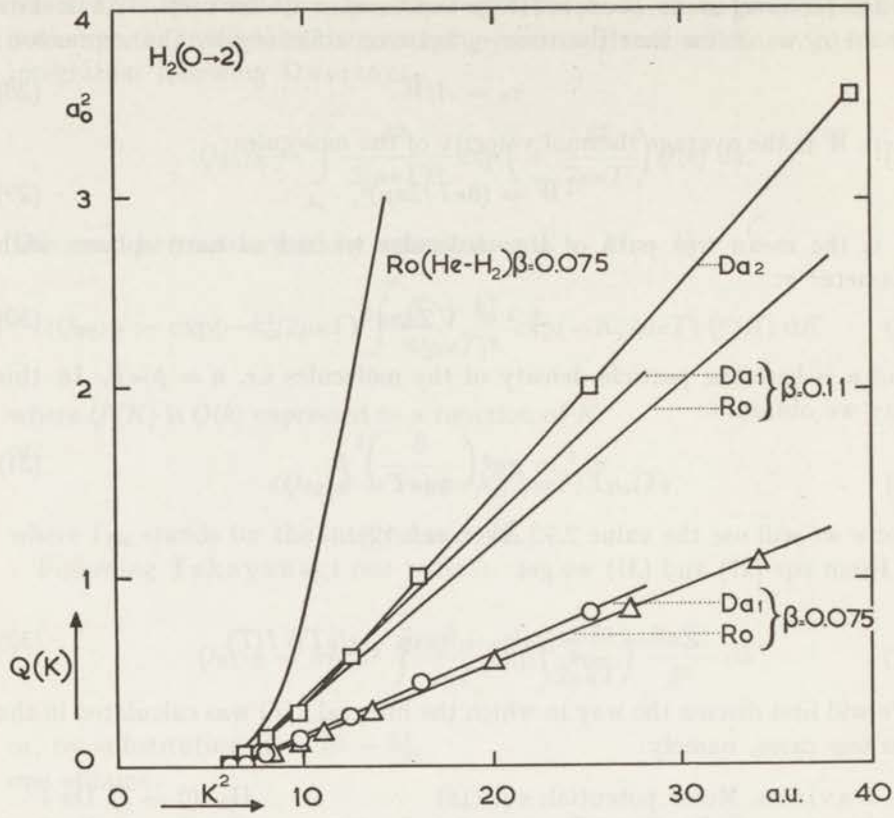

Fig. 3. The collision cross-section for the $0 \to 2$ transition in H_2 as a function of k^2.
○ calculated by Davison using a Morse potential (Da 1)
□ calculated by Davison using an exp.-6 potential (Da 2)
△ calculated by Roberts using a Morse potential (Ro)
Ro(He–H_2) The collision cross-section for the $0 \to 2$ transition in H_2 through collisions with He as calculated by Roberts for a Morse potential.

II we used the approximation:

$$Q(k) = (k^2 - k_0^2)\{c + d(k^2 - k_0^2)\}. \tag{35}$$

To determine c and d $Q(k)/(k^2 - k_0^2)$ is plotted as function of k^2 in fig. 4. As a result we obtained $c = 0.067$ and $d = 0.0036$ $(k_0^2 = 6)$. The error introduced by the approximation at the higher values of k is of little importance, because for high values of k, $M(k)$ rapidly goes to zero so that these values make a negligible contribution to the integral $I(T)$. The integration results in:

$$I_{\mathrm{Da\,2}}(T) = 4c\mu\kappa T\left(1 + \tfrac{1}{2}\frac{k_0^2}{2\mu\kappa T}\right) + 8d(\mu\kappa T)^2\left(3 + \frac{k_0^2}{2\mu\kappa T}\right). \tag{36}$$

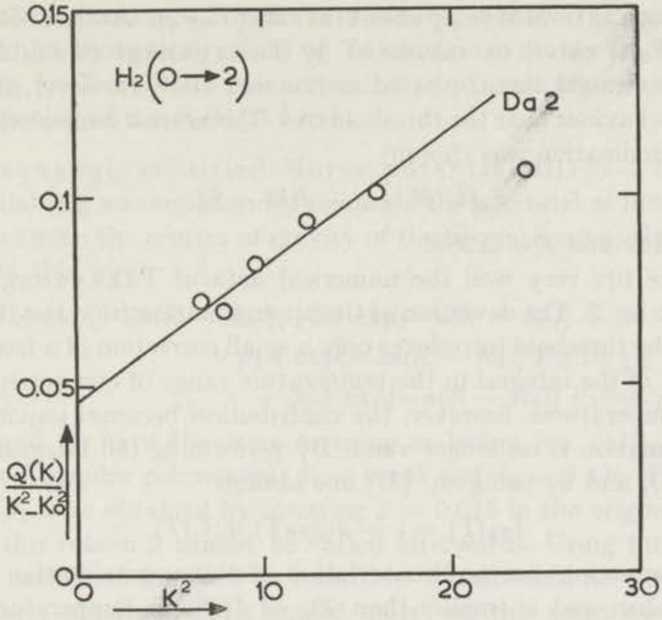

Fig. 4. $Q(k)/(k^2 - k_0^2)$ as a function of k^2 for the $0 \to 2$ transition in H_2(a.u.).
○ calculated by Davison using an exp-six potential
(Da 2). — approximation eq. (35)

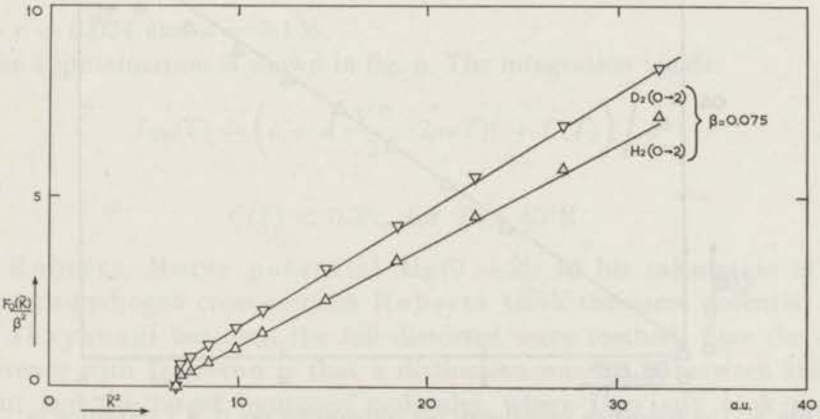

Fig. 5. The transition probability per collision for the $0 \to 2$ transition in H_2 and D_2 as a function of $\tilde{k}^2$.
△ calculated by Takayanagi for H_2
▽ calculated by Takayanagi for D_2
— approximation eq. (37).

c. Takayanagi, Morse potential $H_2\,(0 \rightarrow 2)$. As can be seen in fig. 5, the $F_0(\bar{k})$ curves as calculated by Takayanagi (see table I) give also rise to a straight line if plotted as function of $\bar{k}^2$. However, they show a different behaviour near the threshold of $\bar{k}$. Therefore a somewhat different way of approximation was chosen:

$$F_0(\bar{k})/\beta^2 = c + d(\bar{k}^2 - \bar{k}_0^2) \tag{37}$$

with $c = 0.169$ and $d = 0.265$.

This curve fits very well the numerical data of Takayanagi, as can be seen from fig. 5. The deviation of the approximation from the theoretical curve near the threshold introduces only a small correction of a few per cent in the value of the integral in the temperature range of our measurements. At lower temperatures, however, the contribution becomes important and the approximation is no longer valid. By performing the integration (eqs. (24) and (25)) and by using eq. (37) one obtains:

$$I_{\mathrm{Ta}}(T) = c + d(2\mu\kappa T) + C(T). \tag{38}$$

$C(T)$ is a correction due to the deviation of the approximation near the threshold value, and is smaller than 2% of $I(T)$ for temperatures above 70°K.

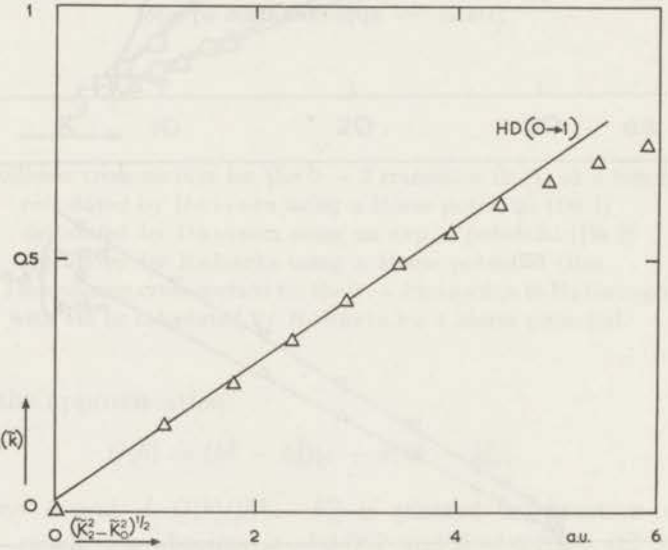

Fig. 6. The transition probability per collision for the $0 \rightarrow 1$ transition in DH as a function of $(\bar{k}_2^2 - \bar{k}_0^2)^{\frac{1}{2}}$.
△ calculated by Takayanagi
— approximation eq. (40).

d. Takayanagi, Morse potential $D_2\,(0 \rightarrow 2)$. Here the same procedure was followed as for H_2. Again eq. (37) was used, the constants now take the values $c = 0.51$ and $d = 0.308$. Fig. 6 shows the approximation made and the theoretical values of Takayanagi (table I). In this case $C(T) < 5\%$ for $T > 70°\mathrm{K}$. This correction arose again from the differences at the beginning of the $F_0(\bar{k})/\beta^2$ curve.

e. Takayanagi, modified Morse potential HD (0 → 1). For HD the potential (13) was transformed to obtain the potential as function of the distance between the centres of gravity of the two molecules. Takayanagi obtained in this way:

$$\begin{aligned} V(R,\chi) = A\exp\{-2\alpha(R-R_0)\} - 2A\exp\{-\alpha(R-R_0)\} + \\ + \beta_1 A\exp\{-2\alpha(R-R_0)\}\,P_1(\cos\chi_1) - \\ - \beta_2 A\exp\{-\alpha(R-R_0)\}\,P_1(\cos\chi_1) \end{aligned} \qquad (39)$$

where A and R_0 have the same meaning as before (eq. (13)), P_1 $(\cos\chi_1)$ is the first Legendre polynomial, $\beta_1 = 0.445$ and $\beta_2 = 0.436$. These values of β_1 and β_2 were obtained by inserting $\beta = 0.075$ in the original potential (13). For this reason β cannot be varied afterwards. Using this potential, $F_0(\bar{k})$ was calculated for the 0 → 1 and 1 → 2 transition. As a result values of $F_0(\bar{k})$ were obtained which exceed unity. As this quantity should not exceed unity this means that the method of approximation used by Takayanagi becomes invalid. Takayanagi therefore corrected his values of $F_0(\bar{k})$ by taking a new $F_0(\bar{k})$ which is defined by $F_0(\bar{k})/(1 + F_0(\bar{k}))$. This corrected value was used in our calculations (see table I). Here we approximated:

$$F_0(\bar{k}) = c + d\sqrt{k^2 - k_0^2} \qquad (40)$$

with $c = 0.024$ and $d = 0.136$.

The approximation is shown in fig. 6. The integration yields:

$$I_{\mathrm{Ta}}(T) = \left(c + d\,\frac{\sqrt{\pi}}{2}\,(2\mu\kappa T)^{\frac{1}{2}} + C(T)\right)\Big/\,\beta^2 \qquad (41)$$

with

$$C(T) < 0.3\% \text{ for } T > 40°\mathrm{K}.$$

f. Roberts, Morse potential H_2 (0 → 2). In his calculation of the hydrogen-hydrogen cross-sections Roberts took the same potential (13) as Takayanagi but used the full distorted wave method; here the only difference with Davison is that a distinction was made between the incident and the target hydrogen molecules, where Davison took proper account of the identity of the two hydrogen molecules. However, as is stated by Roberts his results for hydrogen are in substantial agreement with those of Davison. In this case $Q(k)$ (see table III) was approximated in the same way as had been done for the $Q(k)$ data derived by Davison for the Morse potential (*a*). Here the constant c in eq. (33) takes the value $c = 0.040$ $(\beta = 0.075)$.

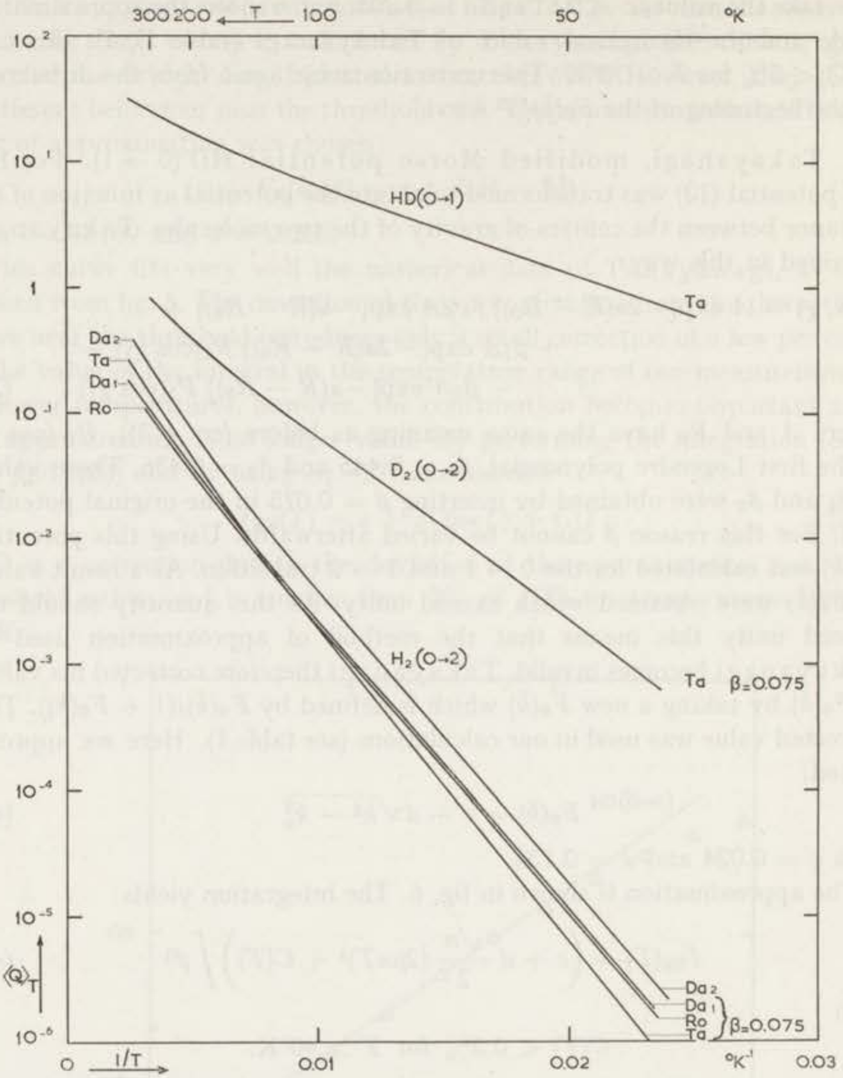

Fig. 7. $\langle Q \rangle_T$, the avaraged collision cross-section in a.u. as a function of $1/T$ for $H_2(0 \rightarrow 2)$, $D_2(0 \rightarrow 2)$ and HD$(0 \rightarrow 1)$.

Having obtained equations for $I(T)$ in the cases $a - f$ it is now possible by using eqs. (26), (27) and (32) to calculate $\langle Q \rangle_T$, τ and Z as functions of temperature. We will first discuss the behaviour of the quantities $\langle Q \rangle_T$, τ and Z by inspection of eqs. (26), (27) and (32) respectively. From eq. (26) it follows that the temperature dependence of $\langle Q \rangle_T$ arises from two factors, $I(T)$ and $\exp(-\varepsilon/\kappa T)$. It can be seen in all cases $a - f$ that $I(T)$ is not strongly temperature dependent. Therefore the temperature dependence of $\langle Q \rangle_T$ arises mainly from the influence of the exponential term in eq. (26),

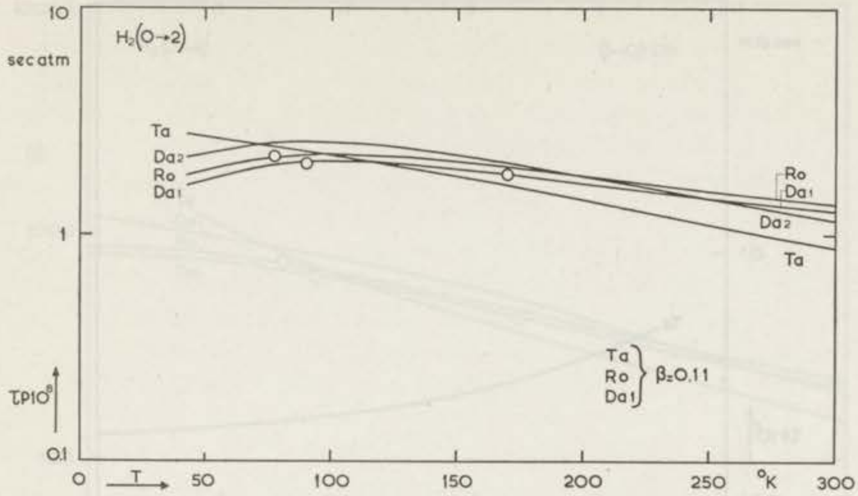

Fig. 8. τp as a function of T for the $0 \rightarrow 2$ transition of H_2.
— theoretical curves
○ experimental points

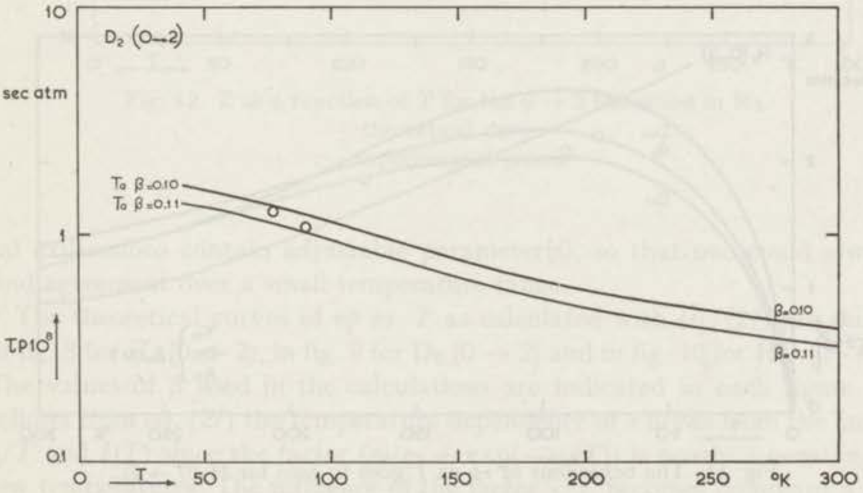

Fig. 9. τp as a function of T for the $0 \rightarrow 2$ transition in D_2.
— theoretical curves
○ experimental points

which in turn originates from the energy distribution of the colliding particles. This is illustrated in fig. 7, where the calculated values of $\langle Q\rangle_T$ are plotted as function of $1/T$ on a semilogarithmic scale (a value of $\beta = 0.075$ was used in those cases were β is variable). One can see in fig. 7 that the calculated curves do not deviate much from the straight line that

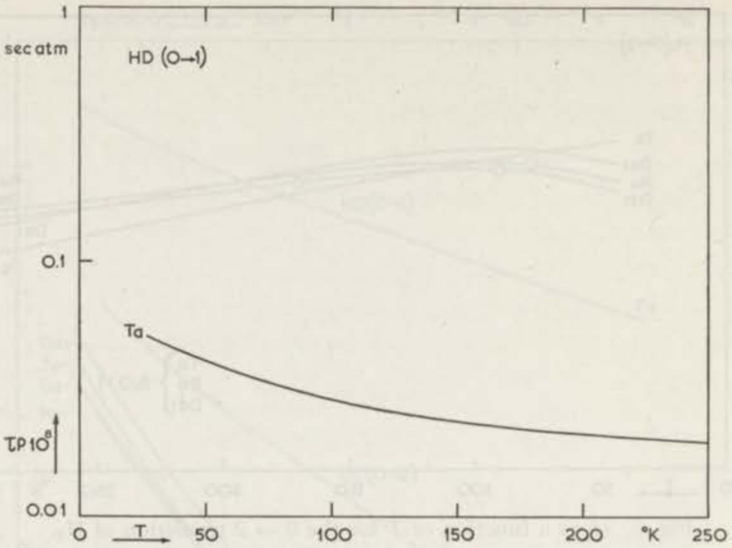

Fig. 10. τp as a function of T for the 0 → 1 transition in HD.
— theoretical curve

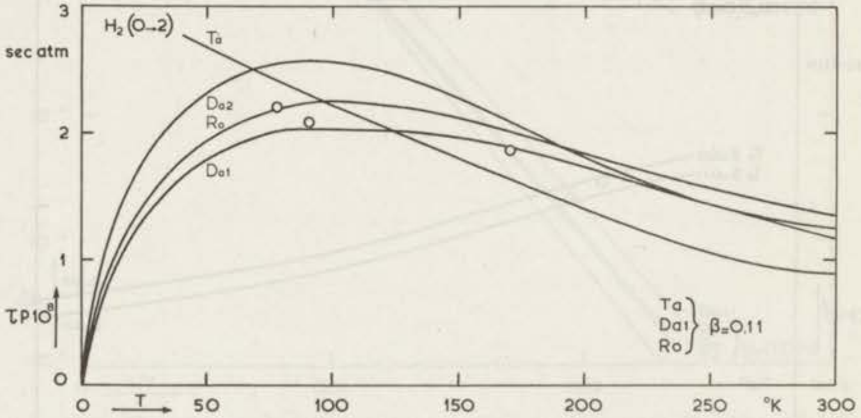

Fig. 11. The behaviour of τp as T goes to zero for $H_2(0 \rightarrow 2)$.
— theoretical curves
○ experimental points

would be obtained if $I(T)$ were a constant. Therefore $\langle Q \rangle_T$ is not the right quantity to consider when comparing the theoretical values with those derived from the experimental determined relaxation times as a function of temperature, because to first order only an affirmation of the trivial exponential temperature dependence will be found. This comparison of theory and experiment as a function of temperature is essential as the theoreti-

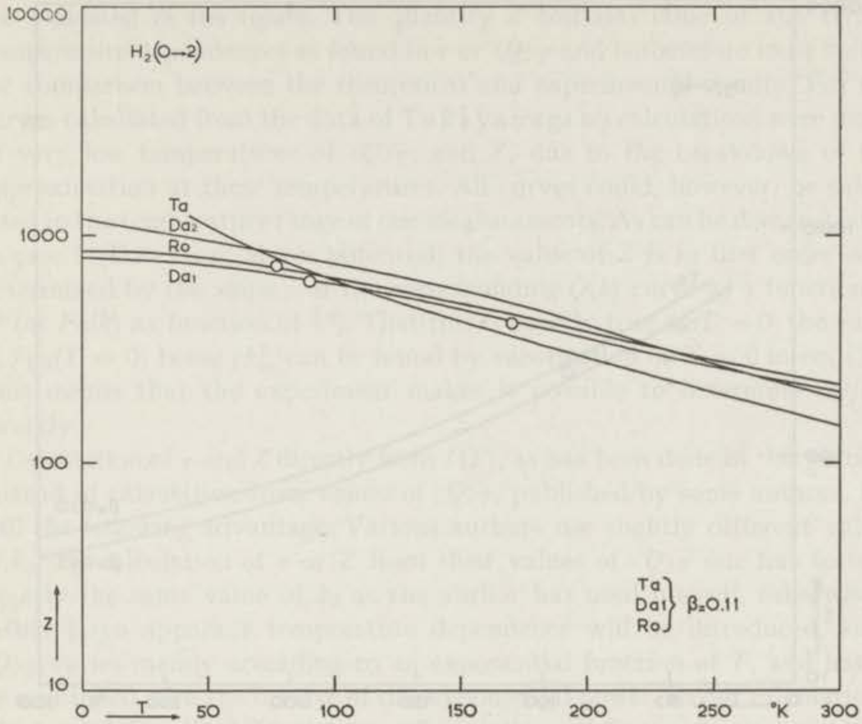

Fig. 12. Z as a function of T for the $0 \rightarrow 2$ transition in H_2.
— theoretical curve
○ experimental points

cal expressions contain adjustable parameter(s), so that one could always find agreement over a small temperature range.

The theoretical curves of τp *vs.* T as calculated with eq. (27) are shown in fig. 8 for H_2 $(0 \rightarrow 2)$, in fig. 9 for D_2 $(0 \rightarrow 2)$ and in fig. 10 for HD $(0 \rightarrow 1)$. The values of β used in the calculations are indicated in each figure. As follows from eq. (27) the temperature dependence of τ arises from the factor $\sqrt{T}$ and $I(T)$ since the factor $(g_0/g_2 + \exp(-\varepsilon/\kappa T))$ is nearly a constant at low temperatures. The influence of the factor $\sqrt{T}$ becomes dominant a low temperature (see fig. 11 for $H_2(0 \rightarrow 2)$), causing τp to go to zero if T goes to zero, since $I(T)$ remains finite in the limit of $T = 0$ (It must be noted that at very low temperatures the rotational specific heat is nearly zero and therefore these relaxation times cannot be determined at all at these temperatures, as the excess sound absorption due to the relaxation becomes negligible with respect to the classical sound absorption). Finally the temperature dependence of Z is only determined by the factor $I(T)$, see eq. (32). The theoretical curves of Z *vs.* T are given in fig. 12 for $H_2(0 \rightarrow 2)$ in fig. 13 for $D_2(0 \rightarrow 2)$ and in fig. 14 for HD $(0 \rightarrow 1)$. The values of β used

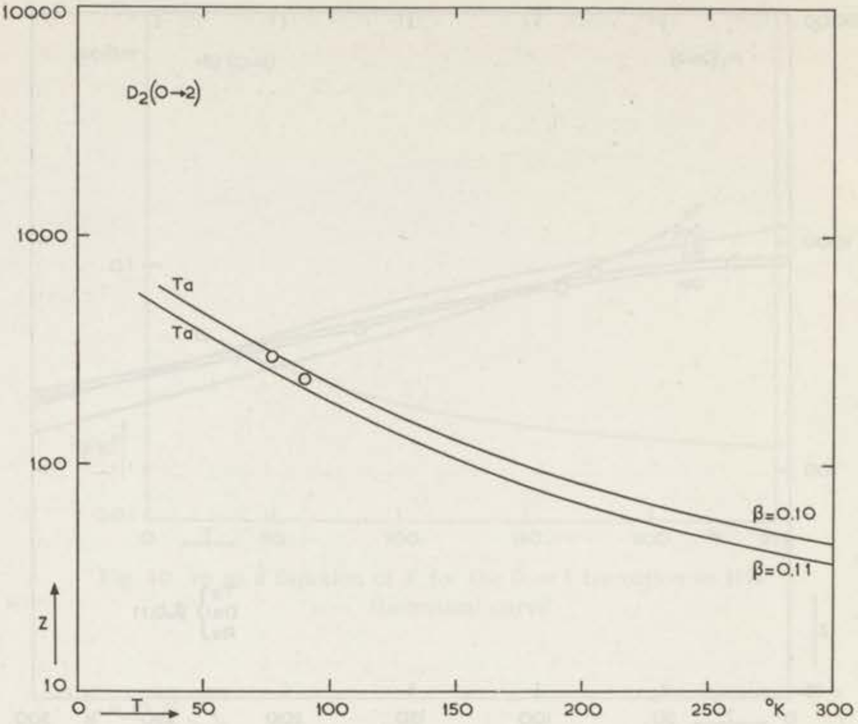

Fig. 13. Z as a function of T for the $0 \rightarrow 2$ transition in D_2.
— theoretical curves
○ experimental points

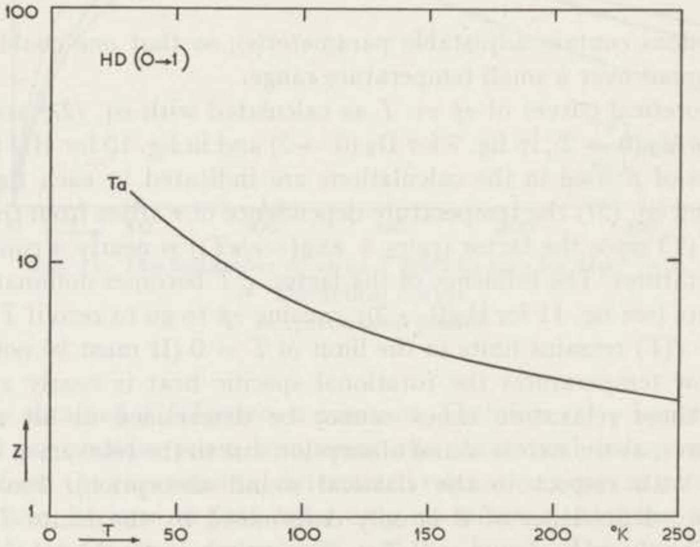

Fig. 14. Z as a function of T for the $0 \rightarrow 1$ transition in HD.
— theoretical curve

are indicated in the figure. The quantity Z contains none of the trivial temperature dependences as found in τ or $\langle Q\rangle_T$ and is therefore most suited for comparison between the theoretical and experimental results. For the curves calculated from the data of Takayanagi no calculations were made at very low temperatures of $\langle Q\rangle_T$, and Z, due to the breakdown of the approximation at these temperatures. All curves could, however, be calculated in the temperature range of our measurements. As can be demonstrated in case a (Davison, Morse potential) the value of Z is in first order only determined by the slope c of the corresponding $Q(k)$ curve as a function of k^2 (or $F_0(\bar{k})$ as function of $\bar{k}^2$). That this is exactly true at $T = 0$, the value of $I_{\mathrm{Da}}(T = 0)$ being ck_0^2, can be found by substitution of $T = 0$ in eq. (34). This means that the experiment makes it possible to determine $\mathrm{d}Q/\mathrm{d}k^2$ directly.

Calculation of τ and Z directly from $I(T)$, as has been done in this section, instead of calculation from values of $\langle Q\rangle_T$, published by some authors, has still the following advantage. Various authors use slightly different values of k_0. By calculation of τ or Z from their values of $\langle Q\rangle_T$ one has to take exactly the same value of k_0 as the author has used himself, otherwise a rather large apparant temperature dependence will be introduced, since $\langle Q\rangle_T$ varies mainly according to an exponential function of T, and has to be multiplied with the inverse of this exponential power. In our calculations, which used directly $I(T)$, these small variations of k_0 are of no importance.

5. Experimental results and discussion. In Chapter I[1]) the experimental $(f/p)_{\max}$ values were communicated for p–H_2 and o–D_2 at 77 and 90°K. These results are shown in table IV together with the result of measurements on the sound absorption of p–H_2 at 170°K, which are given in chapter II[2]). From these $(f/p)_{\max}$ values τ', τ and Z were calculated. From a comparison of the experimental and theoretical results a value is obtained of the adjustable parameter β that was introduced in the Morse potential (13) or (16). These values of β are also given in table IV. From this followed in all cases (Takayanagi, Davison and Roberts)

TABLE IV

Experimental results								
gas	T °K	$(f/p)_{\max}$ MHz/atm	$\tau' p$ 10^{-8}s atm	τp 10^{-8}s atm	$\tau_c p$ 10^{-10}s atm	Z	β_{Ta} $R_e = 6.4$	β_{Da}
p–H_2	77	8.1	1.97	2.20	0.308	717	0.116	0.105
	90	9.3	1.71	2.08	0.331	628	0.116	0.111
	170	13.5	1.18	1.87	0.455	411	0.103	0.110
o–D_2	77	19.5	0.815	1.28	0.433	296	0.104	–
	90	23.0	0.691	1.09	0.469	232	0.107	–

a value of $\beta = 0.11 \pm 0.05$. Therefore the theoretical curves of τ and Z (figs 8, 9, 11, 12 and 13) were calculated for this value of β. The experimental points are indicated in the respective figures. It can be seen that for $H_2(0 \rightarrow 2)$ the experimental points coincide with the theoretical curves over a substantial temperature range. The theoretical curve derived from the cross-sections calculated by Davison for the Morse potential gives the best fit to the experimental points. For $D_2(0 \rightarrow 2)$ conclusions about the temperature dependence cannot yet be drawn as in this case the temperature range of our measurements is not large enough. Concerning the calculations on HD, one can see (fig. 10) that the theoretical value of the relaxation time is much smaller than the corresponding one of p–H_2. This is in accordance with our measurements. The $(f/p)_{max}$ value of HD at 77°K proves to be much larger than the $(f/p)_{max}$ value of p–H_2 at 77°K, the maximum of the absorption curve of HD falls even outside our range of measurement (see figs. 14 and 21, chapter I). We hope to extend the range of our apparatus to higher (f/p) values in order to perform complete measurements on HD. As the $Q(k)$ curve calculated by Roberts[9]) for the transition $(0 \rightarrow 2)$ in a He–H_2 collision is much steeper than the corresponding curve for a H_2–H_2 collision (see fig. 3) the expected relaxation time will now be shorter and hence the $(f/p)_{max}$ values larger than in the case of pure p–H_2. Enlarging the (f/p) range makes it also possible to investigate mixtures of p–H_2 and He.

Overall the following conclusions can be drawn. All theoretical calculations of the cross-section give a fairly good description of the behaviour of the relaxation phenomena in p–H_2, o–D_2 and HD. In the case of p–H_2 and o–D_2 there is good quantitative agreement, while for HD only qualitative agreement has been obtained to date. To extend the comparison between theory and experiment, measurements have to be performed below 77°K especially for o–D_2 and HD. To this end a gas thermostat has been built to be used for measurements between 20 and 77°K.

We will now compare our results with those of other authors. The excess absorption in hydrogen due to the rotational relaxation was detected by Van Itterbeek and Mariens[13]), who found the absorption to exceed the classical value. Stewart and Stewart[14]) and others[15])[16]) made absorption measurements on n–H_2 or n–D_2 at about 293°K. Dispersion measurements were made by Stewart and coworkers[17]). Rhodes[18]) investigated the dispersion in p–H_2 at 197°K in order to deal with a one relaxation-time system. From all these measurements no accurate determination of the relaxation time τ_{02} is possible. Their merit is to indicate a relaxation frequency of the order of 10–12 MHz and to give satisfactory support to the theory of relaxation of the rotational degrees of freedom as is discussed in detail by Markham *e.a.*[19]). Sessler[20]) made therefore careful absorption measurements on n–H_2 at 293°K. To analyze his experimental results he made several assumptions 1° $\tau_{02}/\tau_{13} = 1/1.5$, 2° $\tau_{35} =$

$= \tau_{13}$, 3° the transitions $2 \rightarrow 4$ and $3 \rightarrow 5$ occur independently of the reaction $0 \rightarrow 2$ and $1 \rightarrow 3$ respectively. He then deduces from his measurements $\tau_{02} = 1.29 \times 10^{-8}$ s. Although it is doubtful whether the assumptions made by Sessler are valid, his value of τ_{02} is in accordance with our results for we read from fig. 8 a value of $\tau_{02}p = 1.3 \times 10^{-8}$ s atm. (Da 1, $\beta = 0.11$).

To simplify the problem Geide[21]) investigated p–H_2 at 293°K.

From his experimental absorption- and dispersion curve he obtained a value of $\tau_{02}p = 1.21 \times 10^{-8}$ s atm and $\tau'_{24}p = 2.11 \times 10^{-8}$ s atm. This value of τ_{02} is again in accordance with our results. In deriving his results the assumption 3°, as made by Sessler was made again.

6. Discussion of the measurements on normal hydrogen and normal deuterium at 77°K.

a. n–H_2, 77°K. Normal H_2 is composed of $\frac{3}{4}$o–H_2 and $\frac{1}{4}$p–H_2, which is the equilibrium composition at room temperature. n–H_2 can be treated as a mixture of two distinct gases o–H_2 and p–H_2. As demonstrated by Herzfeld and Litovitz[22]) a mixture of two gases, with each a single relaxation time can be treated exactly as one gas with two internal degrees of freedom excited in parallel. The two relaxation times of this mixture are given in our case by:

$$\tau_1^{-1} = x\tau_{\mathrm{pp}}^{-1} + (1 - x)\,\tau_{\mathrm{po}}^{-1} \tag{42}$$

$$\tau_2^{-1} = x\tau_{\mathrm{op}}^{-1} + (1 - x)\,\tau_{\mathrm{oo}}^{-1} \tag{43}$$

where x is the concentration of the para-component, τ_{pp} is the relaxation time of the p–H_2 in pure para, τ_{oo} of o–H_2 in pure ortho, τ_{po} of one para molecule in pure ortho, and τ_{op} of one ortho molecule in pure para, all relaxation times taken at the total pressure of the mixture. The specific heat of an ortho-para mixture is given by:

$$C_v = x(C_v)_{\mathrm{p}} + (1 - x)(C_v)_{\mathrm{o}} \tag{44}$$

where the upright suffixes p and o refer to the para- and ortho component. Furthermore one has for the rotational specific heats of the mixture:

$$C'_1 = xC''_{\mathrm{p}} \quad \text{and} \quad C'_2 = (1 - x)\,C''_{\mathrm{o}}. \tag{45}$$

It seems reasonable to suppose that in first approximation $\tau_{\mathrm{po}} = \tau_{\mathrm{pp}}$ and $\tau_{\mathrm{op}} = \tau_{\mathrm{oo}}$. This means that in a collision it is irrelevant, whether the colliding particle, which induces a transition, is in an ortho- or a para state. This gives for eqs. (42) and (43) $\tau_1 = \tau_{\mathrm{pp}}$ and $\tau_2 = \tau_{\mathrm{oo}}$. The absorption curve for a process with two relaxation times τ_1 and τ_2 can be written following Herzfeld and Litovitz[22]):

$$\alpha'/f = \left(\frac{V_0}{V}\right)^3 \frac{\pi}{V_0}\,\frac{\Delta}{C_p(C_v - C')}\left\{\frac{C''_1\omega\tau''_1}{1 + \omega^2\tau''^2_1} + \frac{C''_2\omega\tau''_2}{1 + \omega^2\tau''^2_2}\right\}. \tag{46}$$

For the dispersion curve they write:

$$\left(\frac{V}{V_0}\right)^2 = 1 + \frac{\Delta}{C_p(C_v - C')}\left\{\frac{C''_1\omega^2\tau_1''^2}{1+\omega^2\tau_1''^2} + \frac{C''_2\omega^2\tau_1''^2}{1+\omega^2\tau_2''^2}\right\} \qquad (47)$$

C_p and C_v have again the usual meaning, $\Delta = C_p - C_v$.

The quantities C''_1, C''_2, τ''_1 and τ''_2 are defined through the following set of equations:

$$\tau''_{1,2} = \tfrac{1}{2}\left\{\frac{C_v - C'_1}{C_v}\tau_1 + \frac{C_v - C'_2}{C_v}\tau_2\right\} \pm$$

$$\pm \tfrac{1}{2}\left\{\left(\frac{C_v - C'_1}{C_v}\tau_1 - \frac{C_v - C'_2}{C_v}\tau_2\right)^2 + 4\,\frac{C'_1C'_2}{C_v^2}\,\tau_1\tau_2\right\}^{\frac{1}{2}} \qquad (48)$$

$$C''_1 + C''_2 = C'_1 + C'_2 \qquad (49)$$

$$C''_1\tau''_1 + C''_2\tau''_2 = \left(1 - \frac{C'_1 + C'_2}{C_v}\right)(C'_1\tau_1 + C'_2\tau_2) \qquad (50)$$

At 77°K the rotational specific heats of p–H_2 and o–H_2 are 0.30 R and 0.00 R (see Farkas[23])). This gives $C'_1 = \frac{1}{4}C'_p = 0.08\,R$ and $C'_2 = \frac{3}{4}C'_o = 0.00\,R$. The relaxation time $\tau_1 = \tau_{pp} (= \tau_{02})$ at 77°K has been determined from the measurements on pure p–H_2 at 77°K (see table IV).

To calculate the absorption curve all data except τ_2 are available. From $C'_2 = 0$ follows $C''_2 = 0$, hence τ''_2 does not enter into the equations (46) and (47), and we get (see eq. (46)) a one-relaxation-time absorption curve. This absorption curve has a maximum that is about $\frac{1}{4}$ of the maximum of the p–H_2 absorption curve. It must be noted that though for this process τ_{pp} is equal to τ_{02}, $(f/p)_{max}$ differs owing to the different values of the rotational specific heats of n–H_2 and p–H_2. The theoretical absorption curve for n–H_2 and p–H_2 at 77°K together with the experimental points for n–H_2 at 77°K[1]) is given in fig. 15. A reasonable agreement is obtained.

b. n–D_2 at 77°K. n–D_2 is a mixture of $\frac{2}{3}$o–D_2 and $\frac{1}{3}$p–D_2. The same procedure can be followed as was done before n–H_2. From the specific heat data of the deuterium modification as given by Farkas[23]), we obtain: $C'_1 = \frac{2}{3}C'_o = 0.96\,R$ and $C'_2 = \frac{1}{3}C'_p = 0.09\,R$. Again assuming $\tau_{po} = \tau_{pp}$ and $\tau_{op} = \tau_{oo}$ we have:

$$\tau_1 = \tau_{oo} = \tau_{02} \quad \text{o–}D_2(0 \rightarrow 2)\ 77°\text{K}$$

$$\tau_2 = \tau_{pp} = \tau_{13} \quad \text{p–}D_2(1 \rightarrow 3)\ 77°\text{K}.$$

τ_{02} is known from our experiments on pure o–D_2 at 77°K (table IV). τ_{13} may be calculated from the data on the collision cross-section of Takayanagi for the 1 → 3 transition of D_2 (table I), taking again the experimentally derived value of $\beta = 0.11$ and $R_c = 6.4$. In the same way as was done in

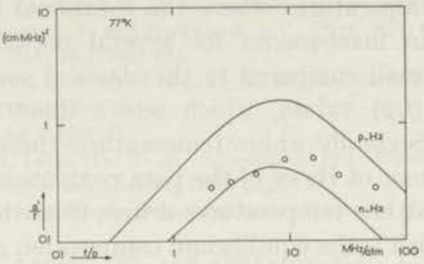

Fig. 15. α'/f as a function of f/p for n–H_2 and p–H_2 at 77°K.
— calculated curves
○ experimental points (n–H_2, 77°K)

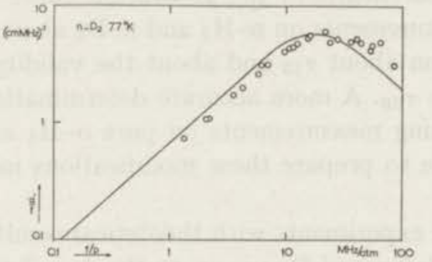

Fig. 16. α'/f as a function of f/p for n–D_2 at 700°K.
— calculated curve
○ experimental points

section 3 for the integration we may use the approximation:

$$F_0(\bar{k})/\beta^2 = a + b(\bar{k}^2 - \bar{k}_0^2) + c(\bar{k}^2 - \bar{k}_0^2)^2 \tag{51}$$

with $a = 0.100$, $b = 0.0773$ and $c = 0.00395$. From this we have $\tau_{13}p = 2.31 \times 10^{-8}$ s atm at 77°K.

Using the system of equations (48), (49) and (50) for two systems in parallel, we get:

$$\tau_1''p = 2.24 \times 10^{-8}\ \text{s atm} \qquad C_1'' = 1.04\,R$$
$$\tau_2''p = 0.79 \times 10^{-8}\ \text{s atm} \qquad C_2'' = 0.01\,R.$$

From these data the absorption curve was calculated using both eqs. (46) and (47). The curve is shown in fig. 16 together with the experimental data. This curve has again nearly the shape which follows from a one relaxation process, owing to the fact that $C_1'' \gg C_2''$. The contribution of the second process is only a small shift of the relaxation time from the value that would be obtained if the first process occurred alone. The agreement between the theoretically derived and the experimentally determined absorption curves is reasonable, taking into account the fact that absorption measurements at temperatures where the rotational specific heat is very small are subject to inaccuracies for several reasons. Firstly, at these temperatures α' is small compared to the classical sound absorption α_{class} especially at high (f/p) values, which sets a limit to the experimental determination of α'. Secondly, at low temperatures there may be a conversion of the ortho component of H_2 or of the para component of D_2 as the equilibrium composition at low temperatures differs from the composition of the normal mixture, which is the equilibrium composition at room temperature. In this case x changes and hence the specific heats C_1' and C_2' (see eq. (45)). The following conclusions concerning measurements on n–H_2 and n–D_2 can be drawn. Below 90°K resp. 50°K n–H_2 and n–D_2 behave as an apparant two-level gas, with a relaxation time τ_{02}, thus no extra information can be obtained from measurements of the absorption curve of these gases. The only use of the measurements on n–H_2 and n–D_2 above 90°K resp. 50°K is to obtain information about τ_{13} and about the validity of the assumption $\tau_{\mathrm{op}} = \tau_{\mathrm{oo}}$ and $\tau_{\mathrm{po}} = \tau_{\mathrm{pp}}$. A more accurate determination of τ_{13} is however possible by performing measurements on pure o–H_2 and pure p–D_2, as it is nowadays possible to prepare these modifications in pure form (see ref. 24).

To compare these experiments with theoretical results it would be useful to extend the calculations of Davison to the $1 \rightarrow 3$ transition of H_2 and D_2 (and also to the $0 \rightarrow 2$ transition of D_2 to compare these results with our measurements on o–D_2).

REFERENCES

1) Sluijter, C. G., Knaap, H. F. P. and Beenakker, J. J. M., Commun. Kamerlingh Onnes Lab., Leiden No. 337*c*; Physica **30** (1964) 745; This thesis, Chapter I.
2) Sluijter, C. G. and Jonkman, R. M., Physica to be published; This thesis, Chapter II.
3) Kneser, H. O., Hb. Physik XI/I (1961).
4) Takayanagi, K., Prog. theor. Phys. **8** (1952) 497.
5) Landau, L. D. and Lifshitz, E. M., Statistical Physics (Pergamon Press, London and Paris, 1959) page 114.
6) Mott, N. F. and Massey, H. S. W., Theory of atomic collisions (Oxford Univ. Press, New York, 1949).
7) Takayanagi, K., Sc. Repts. Saitama Univ. A III (1959) 2.
8) Davison, W. D., Disc. Far. Soc. **33** (1962) 71.
9) Roberts, C. S., Phys. Rev. **131** (1963) 209.
10) Takayanagi, K., Suppl. Prog. theor. Phys. **25** (1963) 1.
11) Condon, E. U. and Shortley, G. H., Theory of atomic spectra (University Press, Cambridge, 1935).
12) Hirschfelder, J. O. Curtiss, C. F. and Bird, R. B., Molecular theory of gases and liquids (John Wiley and Sons, New York, 1954).
13) Van Itterbeek, A. and Mariens, P., Physica **4** (1937) 609.
14) Stewart, E. S. and Stewart, J. L., J. acoust. Soc. America **24** (1952) 194.
(15 Zartman, I. F., J. acoust. Soc. America **21** (1949) 171.

16) **Parbrook, H. D. and Tempest, W.**, J. acoust. Soc. America **30** (1958) 985.
17) **Stewart, E. S., Stewart, J. L. and Hubbard, J. C.**, Phys. Rev. **68** (1945) 231.
18) **Rhodes, J. E.**, Phys. Rev. **70** (1946) 932.
19) **Markham, J. J., Beyer, R. T. and Lindsay, R. B.**, Rev. mod. Phys. **23** (1951) 353.
20) **Sessler, G.**, Acustica **10** (1960) 176.
21) **Geide, K.** Acustica **13** (1963) 31.
22) **Herzfeld, K. F. and Litovitz, T. A.**, Absorption and dispersion of ultrasonic waves Academic Press, New York and London, 1959) page 137.
23) **Farkas, A.**, Orthohydrogen, Parahydrogen and Heavy Hydrogen (University Press, Cambridge, 1935).
24) **Cunningham, M., Chaplin, D.S. and Johnston, H.L.**, J. am. chem. Soc. **80** (1951) 2382.

SAMENVATTING

In dit proefschrift wordt een onderzoek beschreven naar de energieuitwisseling tussen de translatie- en rotatievrijheidsgraden van gasvormige moleculen. Deze komt tot stand bij de onderlinge botsingen der moleculen. De vertraging die kan optreden bij de energieoverdracht, geeft aanleiding tot een verhoogde geluidsabsorptie. Uit metingen van deze geluidsabsorptie als functie van de frequentie kan de voor deze energieuitwisseling kenmerkende tijd, de relaxatietijd, bepaald worden. In de meeste gevallen vindt men echter dat bij dit proces meer rotatieniveaus betrokken zijn, hetgeen aanleiding geeft tot het optreden van verschillende relaxatietijden. Hierdoor is het dan niet meer mogelijk uit de gemeten absorptiekromme de afzonderlijke relaxatietijden ondubbelzinnig af te leiden.

Bij de waterstofisotopen hebben de rotatieniveaus een grote onderlinge afstand tengevolge van het kleine traagheidsmoment der moleculen. Hierdoor is de relaxatietijd voor de rotatie bij waterstofisotopen betrekkelijk lang. Dit houdt in dat de extra geluidsabsorptie reeds bij lage waarden van de frequentie van de geluidsgolf optreedt en voor meting toegankelijk is. Door de temperatuur van de waterstofisotoop te verlagen wordt bereikt dat slechts de langzaamste rotatietoestanden bezet zijn. Omdat in waterstof en deuterium de overgangen tussen even en oneven rotatietoestanden verboden zijn, kunnen de waterstof- en deuteriumisotopen beschouwd worden als een mengsel van twee gassen, een van moleculen met even rotatietoestanden, parawaterstof en orthodeuterium, en een van moleculen met oneven rotatietoestanden, orthowaterstof en paradeuterium. Door nu een ortho- of paramodificatie bij lage temperatuur te nemen kan men bereiken dat men een gas heeft waarin de moleculen slechts twee rotatietoestanden hebben. In dit geval kan men verwachten dat de absorptiekromme als functie van de frequentie de vorm heeft zoals die voorgeschreven is voor een proces met een enkele relaxatietijd. Uit een dergelijke kromme kan dan op ondubbelzinnige wijze deze relaxatietijd bepaald worden. Voor metingen van deze geluidsabsorptie in gassen werd een in dit proefschrift beschreven methode toegepast.

Voor de overdracht van de energie tussen de moleculen is vooral het asymmetrische deel van de intermoleculaire wisselwerking van belang. Voor verschillende intermoleculaire potentialen zijn berekeningen verricht van de inelastische botsingsdoorsnede voor de energieoverdracht van de translatie naar de rotatievrijheidsgraden. Het verband tussen deze grootheden wordt in dit proefschrift aangegeven, alsmede een methode om uit de numerieke gegevens over deze botsingsdoorsnede, door verschillende auteurs berekend als functie van de energie van het bij de botsing invallende deeltje, de relaxatietijd als functie van de temperatuur te berekenen. Uit de gemeten relaxatietijd kan de sterkte van het asymmetrische deel van de intermoleculaire potentiaal bepaald worden.

In hoofdstuk I wordt eerst een beschrijving van de gebruikte methode gegeven. De geluidsabsorptie wordt met een lopende golfmethode gemeten. Als geluidsgever en -ontvanger worden een condensatormicrofoon en -telefoon gebruikt met vast dielectricum. Deze werden aangepast voor gebruik bij lage temperatuur. De gebruikte opstelling maakt het mogelijk de amplitude van de geluidsgolf automatisch op een logarithmische schaal te registreren als functie van de afstand tussen zender en ontvanger. Daar de amplitude exponentieel afneemt, kan uit de helling van de geregistreerde kromme de absorptiecoëfficient bepaald worden. Deze geluidsabsorptie werd gemeten bij een aantal frequenties tussen ongeveer 100 en 500 KHz als functie van de druk van het gas. Aangetoond wordt aan de hand van de absorptievergelijking dat de door de rotatie-relaxatie veroorzaakte extra absorptie, gedeeld door de frekwentie van de geluidsgolf, alleen een functie is van f/p, de frequentie gedeeld door de druk. De extra geluidsabsorptie wordt verkregen door de gemeten absorptie te verminderen met de klassieke geluidsabsorptie, die veroorzaakt wordt door verliezen tengevolge van warmtegeleiding en de viscositeit van het medium. De meetresultaten worden meegedeeld in het tweede gedeelte van hoofdstuk I. Metingen werden verricht in parawaterstof en orthodeuterium bij 77, 90 en 293°K, en in normale waterstof, normale deuterium en hydrodeuterium (HD) bij 77 en 293°K. Voor parawaterstof en orthodeuterium bij 77 en 90°K werden inderdaad absorptiekrommen gevonden die beschreven kunnen worden met een enkele relaxatietijd. De waarde van f/p van het maximum van de absorptiekrommen op de juiste wijze uitgezet, werd in deze gevallen bepaald. De hoogte van de maxima van deze absorptiekrommen bleek in overeenstemming te zijn met de direct uit de rotatie soortelijke warmte berekende waarde van dit maximum.

In hoofdstuk II worden metingen medegedeeld die verricht werden in parawaterstof bij 170°K. Ook hier werd een kromme gevonden die in overeenstemming is met een proces met een enkele relaxatietijd, zodat $(f/p)_{\max}$ weer bepaald kon worden.

In hoofdstuk III worden de theoretische berekeningen van de botsingsdoorsneden behandeld en aangegeven hoe men uit de numerieke gegevens van de botsingsdoorsnede voor een bepaalde rotatieovergang als functie van de energie van het invallende deeltje de relaxatietijd kan berekenen. Verder wordt aangetoond, dat een goede vergelijking tussen de theoretische en experimentele uitkomsten verkregen wordt door de relaxatietijd te delen door de gemiddelde tijd tussen twee botsingen der moleculen. De aldus verkregen grootheid Z kan worden beschouwd als ongeveer het aantal botsingen dat nodig is voor energieoverdracht tussen de translatie- en rotatievrijheidsgraden. Alleen de temperatuurafhankelijkheid van deze grootheid is zonder meer verbonden met het gedrag van de botsingsdoorsnede $Q(K)$ als functie van de energie van het invallende deeltje. Uit de experimenteel bepaalde relaxatietijden wordt een waarde verkregen van de asymmetrie-parameter, die de sterkte van het asymmetrische deel van de intermoleculaire potentiaal aangeeft. Dit gebeurde voor al die gevallen waarbij de botsingsdoorsnede $Q(k)$ berekend is voor een potentiaal, waarbij deze parameter achteraf gevarieerd kan worden.

Voor parawaterstof, dat in een groter temperatuurgebied gemeten werd, is de overeenstemming tussen de experimenteel gevonden temperatuursafhankelijkheid, verkregen met behulp van de berekeningen van de botsingsdoorsnede $Q(k)$ volgens Davison, zeer goed te noemen.

Voor deuterium zijn dergelijke berekeningen echter nog niet uitgevoerd. Vervolgens werden met behulp van de verkregen resultaten de meer gecompliceerde systemen bij 77°K gevormd, door normale waterstof en deuterium, geanalyseerd om de betreffende in hoofdstuk I vermelde metingen te interpreteren. Tevens werden enige mogelijkheden voor verder theoretisch en experimenteel onderzoek aangegeven.

STELLINGEN

I

In de afleiding van Montgomery en Tidman voor de tweede orde [illegible] van de frequentie van een [illegible] in een [illegible] worden [illegible] geen [illegible] correcties in aanmerking genomen.

Montgomery, D. en Tidman, D. A., Phys. Fluids 7 (1964) 242.

II

Dat [illegible] bij [illegible] van [illegible] een magnetisch moment hebben, is [illegible].

III

Bij de ontwikkeling naar harmonischen van een periodieke functie [illegible] kan [illegible] de afleiding van [illegible] worden.

[illegible]

IV

Voor een akoestische thermometer [illegible].

[illegible]

de energie van het invallende deeltje de relaxatietijd kan berekenen. Verder wordt aangetoond, dat een goede overeenkomst tussen de theoretische en experimentele uitkomsten verkregen wordt door de relaxatietijd [illegible] door de gemiddelde tijd tussen twee botsingen der moleculen. De aldus verkregen grootheid λ kan worden beschouwd als [illegible] het aantal botsingen dat nodig is voor energieoverdracht tussen de translatie- en rotatievrijheidsgraden. Alleen de temperatuurafhankelijkheid van deze grootheid is zonder meer verbonden met het gedrag van de botsingsdoorsnede $Q(E)$ als functie van de energie van het invallende deeltje. Uit de experimenteel bepaalde relaxatietijden wordt een waarde verkregen van de asymmetrie-parameter [illegible] van het anisotrope deel van de intermoleculaire potentiaal [illegible]. Dit geschiedt voor al die gevallen waarbij de botsingsdoorsnede $Q(E)$ berekend is voor een potentiaal, waarin deze parameter [illegible] gevarieerd kan worden.

Voor para-waterstof, dat in een groot temperatuurgebied gemeten werd, is de overeenstemming tussen de experimenteel gevonden temperatuurafhankelijkheid, verkregen met behulp van de berekeningen van de botsingsdoorsnede $Q(E)$ volgens Davison, zeer goed te noemen.

Voor deuterium zijn dergelijke berekeningen echter nog niet uitgevoerd. [illegible] worden met behulp van de [illegible] [illegible] [illegible] complicerende systemen bij [illegible] [illegible] [illegible] [illegible], geanalyseerd en de [illegible] in hoofdstuk I [illegible] te interpreteren. Tevens worden enige mogelijkheden voor verdere theoretisch en experimenteel onderzoek aangegeven.

STELLINGEN

I

In de afleiding van Montgomery en Tidman voor de tweede-orde verschuiving van de frequentie van een electromagnetische golf in een koud electronenplasma worden ten onrechte geen relativistische correcties in aanmerking genomen.

Montgomery, D. en Tidman, D. A., Phys. Fluids **7** (1964) 242.

II

Dat voor parawaterstof bij kamertemperatuur een grotere viscositeitsverandering in een magneetveld optreedt dan voor orthowaterstof, ondanks het feit dat bij parawaterstof 50%, bij orthowaterstof 100% der moleculen een magnetisch moment hebben, is niet onbegrijpelijk.

III

Bij de ontwikkeling naar harmonischen van een periodieke functie met grondfrequentie ω noemen sommige auteurs de term die afhangt van 2ω de eerste harmonische; anderen noemen deze term echter de tweede harmonische. Aan deze laatste naamgeving moet de voorkeur gegeven worden.

e.g. Ostrovskii, L. A., Zh. tekh. Fiz. **33** (1963) 905; Sov. Phys. Techn. Phys. **8** (1964) 679.

e.g. Fokker, A. D., Rekenkundige bespiegeling der muziek (Noorduijn, Gorinchem, 1944) blz. 55.

IV

Voor een akoestische thermometer zijn de in dit proefschrift beschreven transducenten zeer geschikt.

Van Itterbeek, A., Forrez, G., Sluijter, C. G. en Vaes, G., Bulletin International du Froid Annexe 1958–1, 155.

Brickwedde, F. G., Temperature. Its measurement and controll in science and industry, III (Rheinhold Publishing Corporation, New York, 1962) dl. 1 blz. 129.

V

Het niet overeenstemmen van de door Geide uit de geluidsabsorptiekromme bepaalde relaxatietijd voor de 2–4 -rotatieovergang in waterstof en de door Davison berekende inelastische botsingsdoorsnede voor deze overgang kan veroorzaakt worden door het ten onrechte aannemen door Geide van een parallelreactie voor de 0–2 en 2–4 -overgang in waterstof.

Davison, W. D., Disc. Far. Soc. **33** (1962) 71.
Geide, K., Acustica **13** (1963) 31.

VI

De voorwaarde die Dutta Roy geeft voor maximale selectiviteit van een brug van Wien, veroorzaakt een beperking van het aantal mogelijkheden. Hierdoor wordt een mogelijkheid met grotere selectiviteit uitgesloten.

Dutta Roy, S. C., Ind. J. Phys. **5** (1963) 245.

VII

Tegen verhoging van de normale-a' (stemtoon) is een fysisch bezwaar aan te voeren.

Geoffrey Rendall, F., The clarinet (Williams and Norgate Ltd., Londen, 1954) blz. 50.
Nederveen, C. J., Acustica **14** (1964) 227.

VIII

Bij de berekening van de diëlektrische constante van parawaterstof als functie van temperatuur en druk besteedt Corruccini te weinig aandacht aan mogelijke invloed van de rotatie op de polariseerbaarheid.

Corruccini, R. J., Nat. Bur. Stand. Techn. Note 144 (U.S. Department of Commerce, Washington, D. C., 1962).

IX

De berekening door Davison van de inelastische botsingsdoorsnede voor de 0–2 -rotatieovergang in waterstof heeft niet het door hem beweerde voordeel van slechts een parameter, daar ook door hem twee parameters worden gebruikt.

Davison, W. D., Disc. Far. Soc. **33** (1962) 71.

X

De beweerde verbetering van de roestwerende werking van loodmenie door toevoeging van zinkchromaat is aanvechtbaar wegens het optreden van een omzettingsreactie.

Meyer, G., Farbe und Lack **70** (1964) 532.

XI

Het is onjuist de zienswijze van Van der Essen als een definitieve oplossing te beschouwen voor het probleem welke de zeventien provinciën van Nederland waren.

Craeybeckx, J., Algemene Geschiedenis der Nederlanden, IV (De Haan, Utrecht; Standaardboekhandel, Antwerpen, 1952) blz. 111.

Van der Essen, L., Deux mille ans d'histoire (La Presse de Belgique, Brussel, 1947).

XII

Het voorkomen van vrijwel uitsluitend Nederlandse toponiemen op recente Franse topografische kaarten van gedeelten van het Franse Noorderdepartement wijst erop dat deze nog steeds behoren tot het taalbezit aldaar.

Van Duinkerken, A., Ons Erfdeel **6** (1962) no. 2, blz. 6.

e.g. Carte de France, Cassel, 1 : 50.000 (Ministère des Traveaux Publics et des Transports, Parijs, 1958).

XX

De bestaande verklaring van de [illegible]

Het is onjuist de zienswijze van Van der Essen als een definitieve oplossing te beschouwen voor het probleem welke de zeventien provinciën van Nederland waren.

[illegible]

Van der Essen, L., [illegible]

VIII

Bij de berekening van de [illegible] constante van [illegible] als functie van temperatuur en druk heeft Carruthers [illegible] een mogelijke invloed van de rotatie op de [illegible]

[illegible] U.S. Department of Commerce, Washington, D.C.

IX

De berekening door Davison van de [illegible]

Davison, W. D., Disc. Far. Soc. 28 (1958) [illegible]